Minerals Engineering, Volume 111, September 2017, Pages 5-24

Towards large scale microwave treatment of ores: Part 2 – Metallurgical testing

A.R. Batchelor[a]*, A.J. Buttress[a], D.A. Jones[a], J. Katrib[a], D. Way[b], T. Chenje[b], D. Stoll[b], C. Dodds[a], S.W. Kingman[a]

[a] Faculty of Engineering, The University of Nottingham, University Park, Nottingham, NG7 2RD, United Kingdom

[b] JKTech Pty Ltd, 40 Isles Road, Indooroopilly, QLD, 4068, Australia

* Corresponding author. Tel.: +44 (0)115 951 4080; fax: +44 (0)115 951 4115. E-mail address: andrew.batchelor@nottingham.ac.uk (A.R. Batchelor)

Keywords

Microwave; Ore; Copper; Pilot Scale; Comminution; Liberation.

Highlights

- Pilot scale (150t/h) microwave-induced fracture of ores is investigated on three ore types
- Microwave treatment energies in the range 0.3-3kWh/t were tested at up to 200kW power input
- Equivalent liberation could be achieved at a 40-70µm coarser grind
- Specific comminution energy could be reduced by up to 9% at nominal plant grinds
- Throughput could be increased by up to 10% at nominal plant grinds

Abstract

A pilot scale microwave treatment system capable of treating 10-150t/h of material at 10-200kW was designed, constructed and commissioned in order to understand the engineering challenges of microwave-induced fracture of ores at scale and generate large metallurgical test samples of material treated at approximately 0.3-3kWh/t. It was demonstrated that exposing more of the ore to a region of high power density by improving treatment homogeneity with two single mode applicators in series yielded equivalent or better metallurgical performance with up to half the power and one third the energy requirement of that used with a single applicator. Comminution testing indicated that A*b values may be reduced by up to 7-14% and that the Bond Ball Mill Work Index may be reduced by up to 3-9% depending on the ore type under investigation. Liberation analysis of the microwave-treated ore indicated that equivalent liberation may be achievable for a grind size approximately 40-70µm coarser than untreated ore, which is in agreement with laboratory scale investigations reported in the literature at similar or higher doses. Flow sheet simulations further indicated that reduced ore competency following microwave treatment could potentially yield up to a 9% reduction in specific comminution energy (E_{CS}) at a nominal plant grind of P_{80} 190µm, or up to 24% reduction at a grind of P_{80} 290µm, for a microwave energy input of 0.7-1.3kWh/t. Throughput could also be increased by up to approximately 30% depending on grind size, ore type and equipment constraints. To date, approximately 900t of material has been processed through the pilot plant, approximately 300t of which was under microwave power. Metallurgical testing has demonstrated that comminution and liberation benefits are achievable at doses lower than that previously reported in the literature, which allow high throughputs to be sustained with low installed power requirements providing a pathway to further scale-up of microwave treatment of ores.

http://dx.doi.org/10.1016/j.mineng.2017.05.003

1 Introduction

Microwave-induced fracture of ores has been widely cited as a means to address some of the challenges faced by the hard rock metalliferous mining industry, for which stakeholders have identified reducing ore competency prior to energy intensive comminution and improving liberation to enable more efficient separation closer to native grain sizes to be among potential solutions (Daniel and Lewis-Gray, 2011; Drinkwater et al., 2012; Pokrajcic et al., 2009; Powell and Bye, 2009). Investigations on microwave-induced fracture of a variety of ores (including copper sulphide, nickel sulphide, lead-zinc sulphide, gold and iron ores) over the past three decades have demonstrated many potential benefits, including reduced comminution energy, enhanced liberation and increased values recovery during flotation.

Dramatic reductions in ore competency (up to 80%), and improvements in liberation (up to 30%) and flotation recovery (up to 20%) following microwave treatment are typically reported in the literature by studies that use low power density multimode cavities at 2.45GHz (such as a kitchen microwave oven) at low power (<3kW) (Amankwah et al., 2005; Amankwah and Ofori-Sarpong, 2011; Andriese et al., 2011; Andriese et al., 2012; Henda et al., 2005; Kingman et al., 1999; Kingman et al., 2000a, b; Kumar et al., 2006; Kumar et al., 2010; Marion et al., 2016; Omran et al., 2015; Orumwense and Negeri, 2004; Vorster et al., 2001; Walkiewicz et al., 1993; Walkiewicz et al., 1991; Wang and Forssberg, 2005). The residence times were long (>>1s, typically in the order of minutes) for small batch masses of ore (up to 1kg) of typically ball mill feed size material (<20mm). Treatments resulted in high bulk temperatures (typically >100°C) and prohibitively high microwave treatment energy input to the ore (>>5kWh/t, frequently >50kWh/t); it was widely acknowledged by the authors that such high microwave energy inputs could not justify the comminution energy savings using such microwave systems. Furthermore, the long residence times required to achieve these benefits would otherwise not support the high throughputs required by the mining industry (>100t/h).

The encouraging results were not universal and were highly dependent on the mineralogy of the ores tested. The efficacy of the generation of thermally-induced fractures, and thus the amenability of ores to microwave treatment, have been empirically shown to be depend on the dielectric, thermal and mechanical properties of the minerals involved, their assemblage within the ores, and the microwave energy and power density employed. Theoretical studies by several authors have confirmed these observations mechanistically (Ali and Bradshaw, 2009, 2010, 2011; Jones et al., 2005, 2007; Like and Jun, 2016; Salsman et al., 1996; Wang et al., 2008; Wang and Djordjevic, 2014; Whittles et al., 2003). In particular, the theoretical studies suggested that high power densities (typically in the order of $1x10^{8}W/m^{3}$ – $1x10^{11}W/m^{3}$ in the microwave-heating phase) could yield the same amount of microwave-induced fracture at a fraction of the microwave energy input and in a fraction of the time compared to lower power density treatments due to faster heating rates and higher thermal stresses.

Experimentation using high power density single mode applicators at 2.45GHz with higher power (up to 30kW) enabled economically feasible microwave energy inputs (<5kWh/t) with short residence times (<1s) that would support high throughputs. There are few direct comparisons between low power density multimode and high power density single mode cavity experiments in the literature. Kingman et al. (2004a) showed that Point Load Index reductions of approximately 60% could be achieved on a lead-zinc ore using a single mode cavity with <2kWh/t microwave energy input, which was approximately 10-20 times less energy than required in a multimode cavity for an equivalent strength reduction. Kingman et al. (2004b) and Scott et al. (2008) both tested the same copper ore investigated by Kingman et al. (2000a) in a multimode cavity and demonstrated improved liberation after high power density microwave treatments on lump fragments (>10mm) in single mode cavities with up to 15kW microwave power at economically feasible energy inputs (0.1-5kWh/t). Furthermore, Sahyoun et al. (2005) conducted flotation tests on the same ore and demonstrated a 3-6% increase in copper recovery after microwave treatment (up to 12kW and 1.7kWh/t on <22mm size material) as opposed to the 1% increase reported by Kingman et al. (2000a), attributed to the higher power density sustained in the single mode cavity. Treating coarser particles as opposed to ball mill feed size material further ensured that more of the microwave-heating phases are constrained by the non-sulphide gangue matrix, thereby promoting more microwave-induced grain boundary fracture. Other authors have also demonstrated significant reductions in ore competency (up to 40%) (Batchelor et al., 2015; Rizmanoski, 2011) and improvements in liberation and flotation recovery (~1%) (Batchelor et al., 2016) using single mode cavities under economically favourable microwave treatment conditions, though typically at microwave treatment energies >1kWh/t.

Potential paths to scale up were identified by researchers in the field (Bradshaw et al., 2007) and trialled during the AMIRA P879a project and during pre-piloting studies at up to approximately 30t/h (instantaneous) and 30kW (2.45GHz) in batch systems. However, to demonstrate continuous microwave treatment at a scale in the order of that required by the mining industry, it was necessary to build larger single mode cavities by utilizing the 896MHz frequency that could support even higher power output from microwave generators (up to 100kW) to maintain the power densities used at laboratory scale.

http://dx.doi.org/10.1016/j.mineng.2017.05.003

In the first part of this paper (Buttress et al., 2017), a bespoke, laboratory-based, high throughput and continuous pilot scale microwave treatment system capable of treating up to 150t/h of ore with up to 200kW of microwave power was described. The paper details the integration of microwave applicators with materials handling components and ore presentation to provide a stable and reliable treatment that also meets with occupational health and safety (OHS) and electromagnetic compatibility (EMC) regulations. The aim of the facility was to understand and develop know-how surrounding the engineering challenges of microwave-induced fracture at scale, to generate large metallurgical test samples (up to 6t batches) for subsequent analysis and to support project valuation. Following the design and construction phases of the project, commissioning tests, upgrades and metallurgical tests were conducted over a period of two years, during which time approximately 200 recorded test runs were completed on nine different ore types with a total of approximately 900 tonnes of material processed, 300 tonnes of which was under microwave power.

This second part of the paper presents the results of two campaigns of metallurgical testing (herein referred to as Phase I and Phase II) on three different ore types following microwave treatment in the pilot scale system. Phase I employed a single microwave applicator whereas Phase II employed two applicators in series following system upgrades. The pilot scale testing specifically targeted low microwave treatment energy doses (0.3-3kWh/t) to maximise throughtput and investigate the potential comminution and liberation benefits that may be achieved at doses lower than that previously reported in the literature. The specific objectives of each campaign were as follows:

- Understand the effect of dose at fixed power density (variable throughput) using a single microwave applicator.
- Understand the effect of dose and power density at fixed throughput (variable power input) using two applicators in series.
- Understand the effect of treatment homogeneity by comparing the results from single and dual applicator configurations at similar dose and power density conditions.
- Evaluate the potential changes in comminution circuit performance using flowsheet modelling based on laboratory test results.

2 Materials and methods

2.1 Ore samples

The ore samples used throughout the piloting investigation were all sourced from a major porphyry copper mine owned and operated by the project sponsor. Three ore types of differing lithology were selected for the Phase I testing campaign, labelled Ore 1, Ore 2 and Ore 3, with Ores 1 and 2 studied further in the Phase II testing campaign. All three ore types contained chalcopyrite as the dominant copper sulphide mineral and pyrite as the dominant sulphide gangue mineral. Other microwave-heating phases included hydrated smectite clays (classified as montmorillonite) and typically poorly heating iron oxides, such as hematite. Table 1 gives the average modal mineralogy for each sample from liberation testing, discussed further in section 2.2.4, with standard deviation to show the variability obtained across different individual samples. There was good agreement between the two bulk samples taken for Phase I and Phase II testing and little variation between individual samples.

Example texture images were captured using a Mineral Liberation Analyser (MLA) (FEI, 2016a) at the University of Nottingham and are presented in Figure 1. All three ores typically had well disseminated heating phases with little observable association of copper and iron sulphides. However, Ore 3 contained many fragments with veined or otherwise very coarse sulphide mineralisation. Ore 1 also contained infrequent veined or coarse mineralisation.

The grain size distributions of selected minerals were extracted using the MLA and are presented in Figure 2. It can be seen that the copper sulphides have a native grain size D80 of approximately 170-260µm, the iron and other sulphides (including molybendite, and trace galena and sphalerite) have a combined native grain size D80 of approximately 265-715µm, and the other heaters (predominantly iron oxides, titaniferrous iron oxides and montmorillonite) have a native D80 of approximately 55-1,000µm. The nominal plant grind for the host mine is P80 190µm; therefore, the native copper sulphide grain size are up to 70µm coarser than the target grind size.

http://dx.doi.org/10.1016/j.mineng.2017.05.003

Table 1

Phase I and Phase II average modal mineralogy

Modal Mineralogy (%wt)	Phase I						Phase II			
	Ore 1		Ore 2		Ore 3		Ore 1		Ore 2	
Mineral	Ave.	σ	Ave.	σ	Ave.	σ	Ave.	σ	Ave.	σ
Copper Sulphides a	1.48	0.06	1.15	0.04	0.81	0.06	1.48	0.06	1.08	0.05
Iron Sulphides b	0.91	0.05	4.11	0.22	8.46	0.65	0.68	0.04	4.33	0.22
Iron Oxides c	0.19	0.03	0.74	0.06	2.00	0.16	0.26	0.08	0.38	0.13
Quartz	88.95	1.23	35.34	1.67	19.90	1.17	89.10	0.87	37.84	1.72
Feldspar	3.34	1.30	33.14	1.99	20.20	0.60	1.84	0.24	30.08	1.67
Mica-Phyllosilicate d	4.62	1.80	23.11	1.61	3.37	0.43	6.30	0.64	20.78	1.64
Amphibole	0.02	0.01	0.17	0.06	5.04	0.52	0.01	0.01	0.35	0.16
Calcite	0.06	0.04	0.12	0.06	4.63	0.17	0.07	0.04	0.40	0.12
Garnet e	0.05	0.01	0.26	0.16	13.88	0.73	0.01	0.01	0.65	0.36
Pyroxene	0.09	0.03	0.69	0.08	15.72	0.59	0.02	0.02	1.47	0.65
Other	0.28	0.16	1.19	0.12	6.00	0.45	0.24	0.05	2.64	0.35

[a] Predominantly chalcopyrite with minor bornite, covellite and chalcocite.
[b] Predominantly pyrite, including minor molybdenite with trace galena and sphalerite.
[c] Iron Oxides predominantly hematite with some magnetite and Fe/Ti oxides including ilmenite and rutile.
[d] Mica-Phyllosilicate group includes biotite, chlorite, kaolinite, muscovite and montmorillonite.
[e] Garnet classified as andradite.

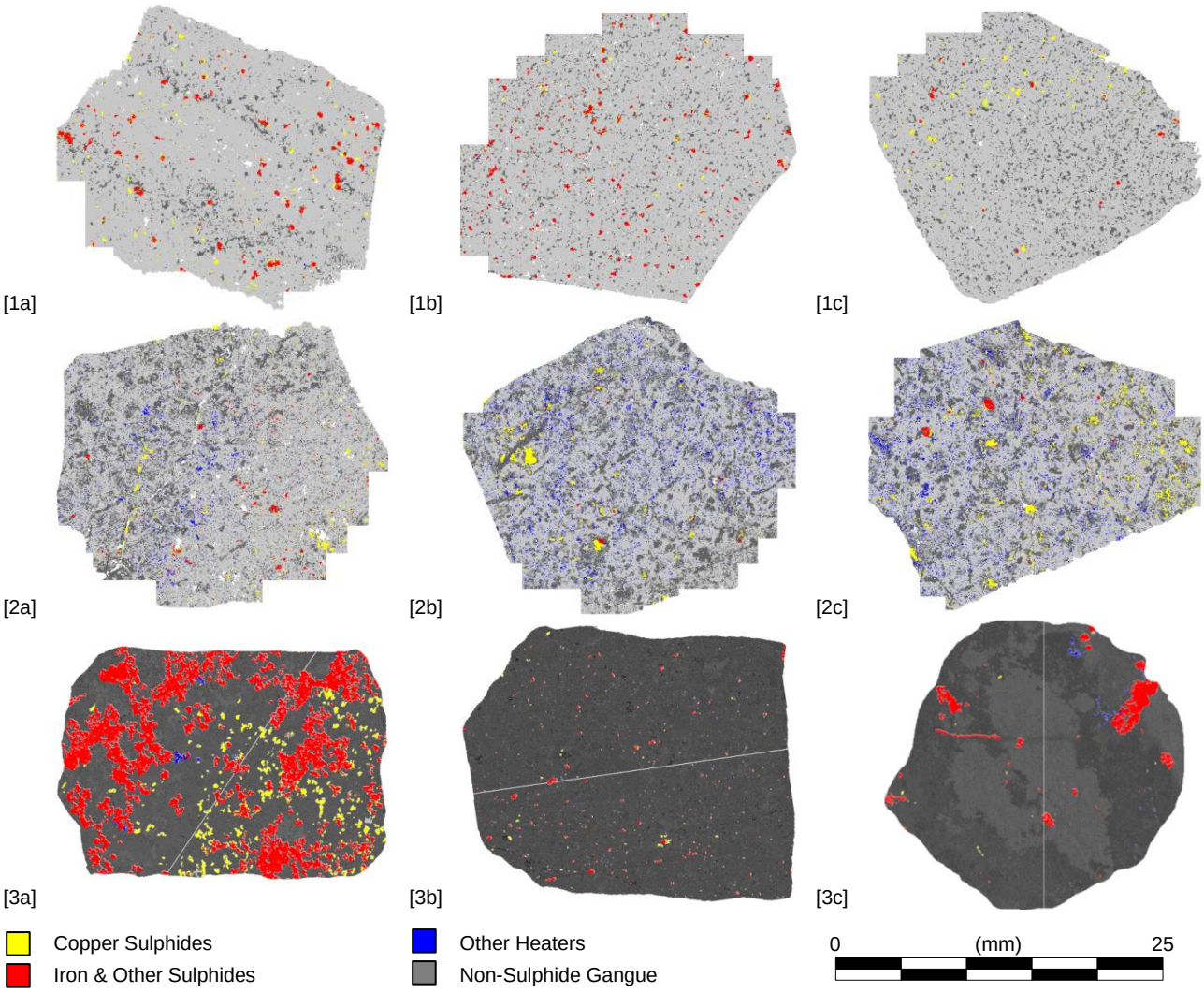

Figure 1: Example lump fragment false colour images from MLA mineralogical texture analysis for Ore 1 (1a-c), Ore 2 (2a-c) and Ore 3 (3a-c)

http://dx.doi.org/10.1016/j.mineng.2017.05.003

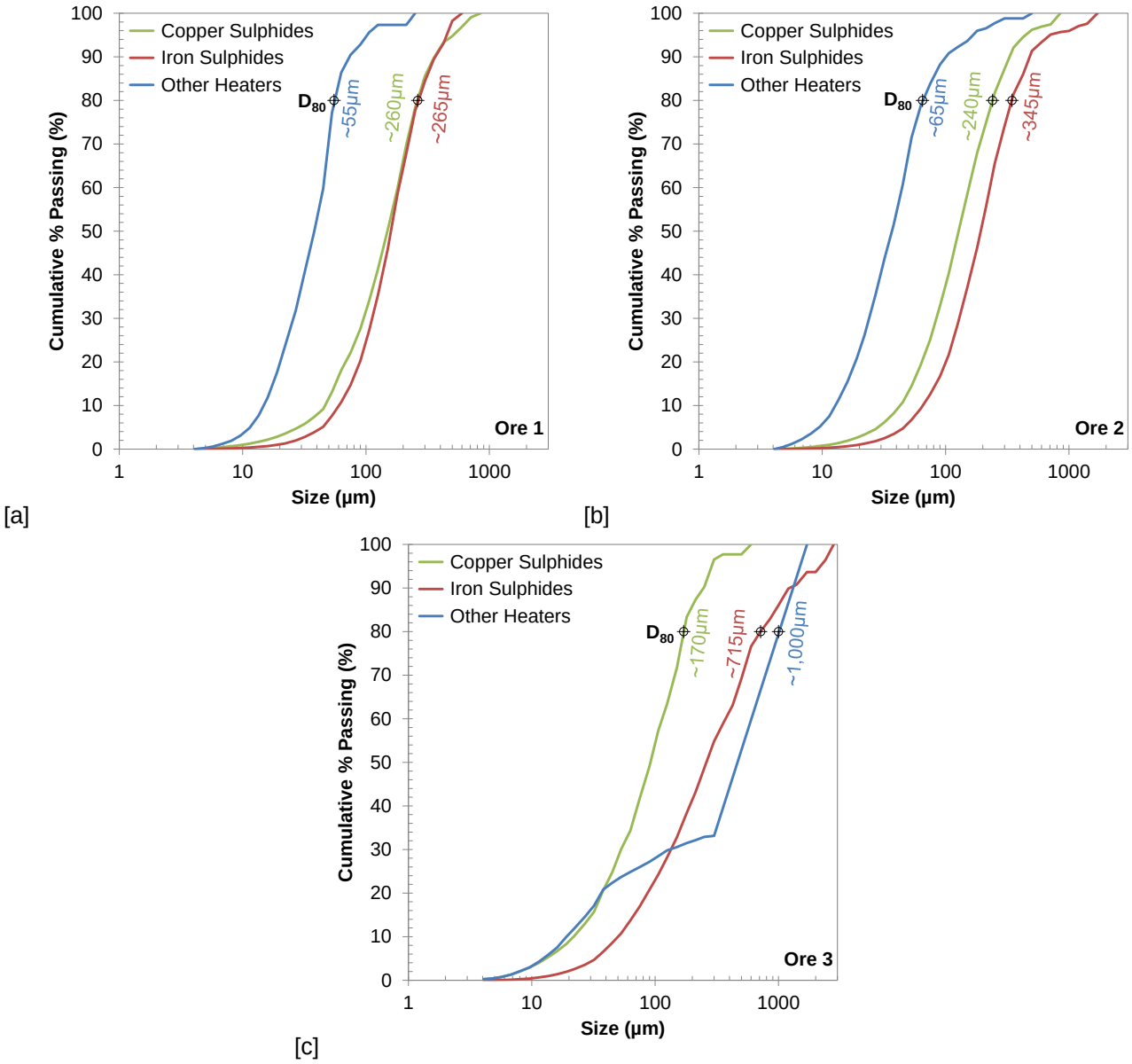

Figure 2: Microwave-heating phase grain size distributions for [a] Ore 1, [b] Ore 2 and [c] Ore 3

A narrow particle size range of nominally -50.8+25.4mm was tested for all three ores. Bulk screening of the ore at the host mine and some breakage during handling resulted in up to approximately 30% of the ore being finer than 25.4mm, illustrated in Figure 3. Coarser fragments would have increased the risk of flow problems in the applicator tube, whereas finer fragments might be expected to return diminishing benefits from microwave treatment as more heating minerals would occur near the surface of the fragments.

Low purity silica sand, which was similar in dielectric properties to the non-sulphide gange minerals in the ore sample, was screened to <6.35mm and used as fines to fluidize the ore material and fill air voids during Phase I testing. This ensured that the microwave energy was mostly absorbed by the ore sample. A sample of the test ore material was subsequently crushed and screened to <6.35mm to provide fines that were similar in dielectric properties to the bulk ore and used for this purpose during Phase II testing. This ensured that Phase II testing mimicked a mass and dielectric loading in the applicator akin to run-of-mine (ROM) ore.

http://dx.doi.org/10.1016/j.mineng.2017.05.003

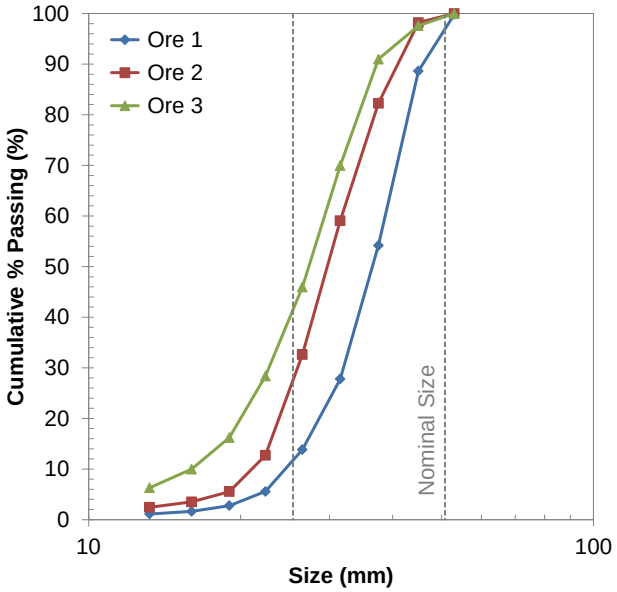

Figure 3: Feed size distributions

2.2 Testing methodology

Several tonnes of each ore type were received at the University of Nottingham facility in a combination of bulk bags and drums. Upon selection of the test matrix, the total weight was taken from the bulk stock. Approximately 750kg per sample was then split by rotary sample divider, ensuring representivity in that the untreated control sample was taken from the same batch of ore as the material to be treated during the current campaign and not separately from the bulk stock. The primer, ore sample and ore fines were charged to the feed bins. The system was primed and the required blends charged to the microwave feed bin A05. The microwave treatment was executed at the chosen conditions and the microwave-treated material collected in the discharge bins. Some partially microwave-treated or untreated ore reported to DB01 with the primer (prior to steady state microwave treatment) and DB03 (left over material in the mass flow hopper after microwave power had been switched off). The metallurgical samples of approximately 500kg were collected from DB02 and comprised only material treated at steady state at the chosen conditions. The primer and ore fines were screened from the ore and recycled during the testing campaigns. The ore fractions from DB01 and DB03 were set aside and only recycled for non-metallurgical testing purposes.

The untreated and microwave-treated samples were sent to JKTech in Brisbane, Australia, for metallurgical analysis. The suite of analyses included the JKGeM Ci test, JK Drop Weight (JKDW) test, Bond Ball Mill Work Index (BBMWi) test and liberation by scanning electron microscopy using QEMScan (FEI, 2016b). The comminution results were also used as inputs into flow sheet modelling by JKSimMet to determine the influence on comminution performance under both constrained and unconstrained conditions based on the ore sample host mine grinding circuit. The constrained and unconstrained conditions were considered to evaluate potential Brownfield and Greenfield applications of microwave treatment.

2.2.1 JKGeM Ci test

The JKGeM Ci test is performed by starvation crushing narrow size classes (e.g. -31.5+26.5mm) of ore at a fixed size reduction ratio of 2.5 (geometric mean particle size to crusher closed side setting). The test produces two indices, defined as CRU and GRD, and the percent passing 4.75mm. The CRU index represents a mass ratio of coarse to fine material generated, which tends to correlate with the impact resistance of the material (note a higher CRU index indicates a beneficial change softer ore). The GRD index represents the normalised slope of the product on a log-log scale and reflects the inherent breakage response of the material (note a lower GRD index indicates a beneficial change softer ore). JK GeM project studies have shown a high level of correlation between this slope and the grindability of the ore, making the GRD index a very useful marker for comparing the ore breakage properties (Kojovic et al., 2010). The JKGeM Ci test methodology has the added advantage of producing a crushed product that can be used for subsequent testing, meaning the test can be logically added into the characterisation flowsheet as a prerequisite to later tests. Thus, the JKGeM Ci test was selected as a rapid coarse particle evaluation tool to replace the Point Load Index test used in earlier published literature on small batch microwave treatments of ore (Batchelor et al., 2015; Kingman et al., 2004a; Kingman et al., 2004b).

http://dx.doi.org/10.1016/j.mineng.2017.05.003

2.2.2 BBMWi test

The BBMWi test (Bond, 1961) was chosen to assess any reduction in ore competency at the grinding stage and to provide the necessary ball mill grinding work index input for flow sheet modelling. The test was conducted by first stage crushing the material to 3.35mm and determining the feed size distribution by sieving. 700mL was charged to a standard Bond batch ball mill and operated at 70rpm with standard ball charge. After 100 revolutions, the mill was emptied and all material finer than the closing screen (P_1) was removed and replaced with fresh feed material. The material was ground for a number of revolutions calculated to produce a 250% circulating load. The material was again removed, screened and the undersize replaced by fresh feed. The cycle was repeated until the undersize produced per revolution reached equilibrium. The average of the net mass per revolution from the last three cycles was taken as the ball mill grindability (Gbp) and the product size distribution determined. The work index was then calculated according to Eq. 1:

$$BBMWi = \frac{49.05}{P_1^{0.23} \times Gbp^{0.82} \times \left(\frac{10}{\sqrt{P_{80}}} - \frac{10}{\sqrt{F_{80}}}\right)} \quad 1$$

where BBMWi is the Bond Ball Mill Work Index (kWh/t), P_1 is the closing test sieve aperture (µm), Gbp is the grindability (g/rev), F_{80} is the 80% passing size (µm) of the feed and P_{80} is the 80% passing size (µm) of the product.

2.2.3 JKDW test

Similarly to the BBMWi test, the JKDW test was chosen to assess any reduction in ore competency and to provide the necessary impact breakage parameter inputs for flow sheet modelling. The test comprises a variable mass steel drop-weight that can be raised and dropped from a range of predetermined heights onto a particle positioned on a steel anvil. A wide range of energy inputs can be achieved by utilising the potential energy of the drop-weight. An ore sample is screened into narrow size classes and each fragment is impacted in turn at set energy inputs. The breakage products are collected and sieved, and the impact breakage parameters A and b calculated from the size distributions and input energies. Due to sample mass constraints, in these investigations a modified JKDW test was performed without replicates on the microwave-treated samples by considering only the -31.5+26.5mm size class. A full JKDW test was performed without replicates on the untreated samples allowing an estimate of the full JKDW test to be calculated for each of the microwave-treated samples.

2.2.4 Liberation

Both the untreated and microwave-treated samples were stage crushed in a laboratory jaw crusher to 3.35mm at the same closed side settings (CSS) and at a controlled rate via a vibrating feeder to ensure the same conditions for breakage. The crusher products were split by rotary sample divider into representative 1kg sub-samples for batch grinding in a laboratory rod mill operated at 65%wt solids and 63% critical speed.

Batch grinds were conducted to achieve a grind size P_{80} of 150µm, plus 360/425µm and 600µm to investigate any change in liberation coarser than the plant grind. The milled samples were then wet and dry screened into the root 2 series for liberation analysis. The sized fractions were set in resin in 30mm diameter mounts and enough mounts were prepared to ensure a minimum particle count of 10,000 particles in each size class. The mounts were then ground, polished and carbon coated to present particle cross sections for scanning electron microscopy using a QEMScan liberation analyser.

2.3 Microwave treatments

Microwave treatments and metallurgical testing were conducted across two campaigns of work. Phase I conducted sighter testing on three ore types with the pilot plant using a single microwave applicator. An untreated sample (UT1) was taken and three microwave treatments performed (T1, T2, T3). Power was fixed at 100kW and throughput varied to vary dose while maintaining power density. Silica sand was used as fines for void control with an ore to fines ratio of 40:60. Subsequently, Phase II conducted testing on two ore types with the dual applicator configuration. A second untreated sample (UT2) was taken and another three microwave treatments performed (T4, T5, T6). Where possible, throughput was fixed at 150t/h and power varied to vary dose and power density. Ore fines were substituted for silica sand for void control to promote a more homogeneous dielectric load in the applicator.

The full treatment conditions for both campaigns of testing are given in Table 2. The selected conditions allowed the influence of power density, dose and treatment homogeneity on ore beneficiation to be investigated. A description of the single and dual applicator configurations, along with a description of the treatment sequence followed during operation of the pilot plant, are given in detail in the first part of this paper (Buttress et al., 2017).

http://dx.doi.org/10.1016/j.mineng.2017.05.003

Table 2

Phase I and Phase II microwave treatment conditions

Test ID	Power (kW)	Throughput (t/h)	Dose (kWh/t)	Average Power Density (W/m³)
Phase I				
Ore 1				
T1	1 x 100	70	1.4	$6.6x10^6$
T2	1 x 100	50	2.0	$6.6x10^6$
T3	1 x 100	30	3.3	$6.6x10^6$
Ore 2				
T1	1 x 100	70	1.4	$6.6x10^6$
T2	1 x 100	50	2.0	$6.6x10^6$
T3	1 x 100	30	3.3	$6.6x10^6$
Ore 3				
T1	1 x 100	70	1.4	$6.6x10^6$
T2	1 x 100	50	2.0	$6.6x10^6$
T3	1 x 100	30	3.3	$6.6x10^6$
Phase II				
Ore 1				
T4	2 x 50	150	0.7 [2 x 0.3]	$3.3x10^6$
T5	2 x 75	150	1.0 [2 x 0.5]	$5.0x10^6$
T6	2 x 100	150	1.3 [2 x 0.7]	$6.6x10^6$
Ore 2				
T4	2 x 50	150	0.7 [2 x 0.3]	$3.3x10^6$
T5	2 x 75	150	1.0 [2 x 0.5]	$5.0x10^6$
T6	2 x 80	120	1.3 [2 x 0.7]	$5.3x10^6$

3 Comminution testing

3.1 Visual observations post-microwave treatment

Through visual inspection of the ores post-microwave treatment it was estimated that between 5 and 20% (by mass) of the fragments contained varying degrees of visible macro-fracture, from fragments cleaved (solely due to microwave treatment) along mineralised planes such as veins, to millimetre length cracks located adjacent to sulphide grains. Intact fragments with large microwave-induced macro-fractures could often be broken apart by hand or with a light tap by a hammer to reveal exposed sulphide mineralisation on the surface of the daughter particles, as illustrated in Figure 4a-f. Such fracture has occurred due to selective heating of the sulphide minerals where the clustering of grains has provided a region particularly susceptible to microwave treatment causing preferential breakage along the mineralised plane.

Further exploratory testing on Ore 3 demonstrated that microwave-induced macro-fractures could be created at even lower doses than those used during the metallurgical testing campaigns. Figure 4g illustrates visible microwave-induced fractures from a dual applicator treatment at 2 x 30kW and 140t/h, yielding a dose of approximately 0.4kWh/t.

3.2 JKGeM Ci test results

The JKGeM Ci test was performed in duplicate during Phase I and subsequently in triplicate during Phase II in order to improve the confidence levels between microwave-treated and untreated material calculated by t-tests, given in Table 3 and Table 4 respectively. An error during testing of Ore 2-T5 meant that only one test, without replicate, was able to be used.

http://dx.doi.org/10.1016/j.mineng.2017.05.003

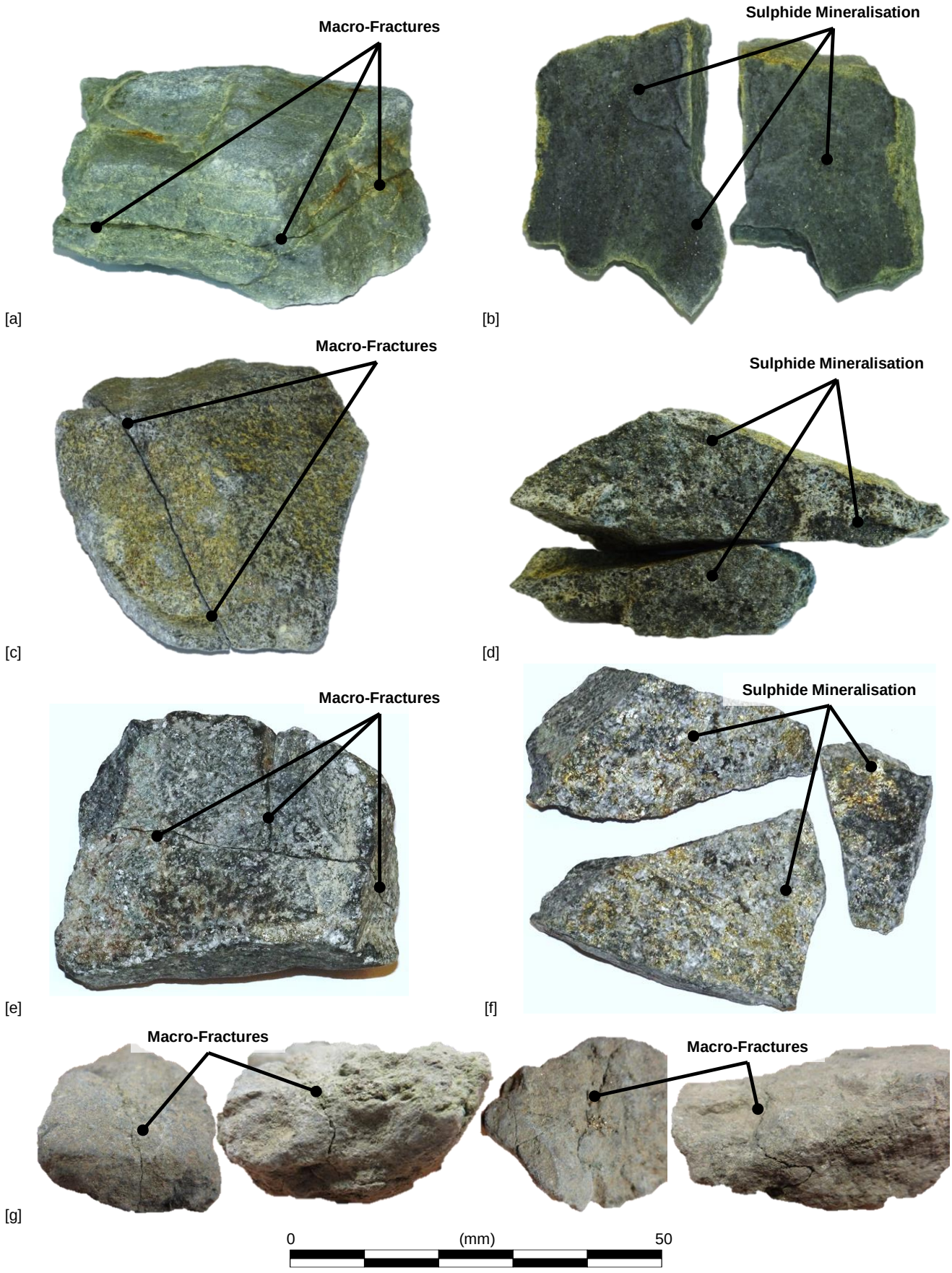

Figure 4: Example images of microwave-induced macro-fractures for intact fragments and after breaking apart by hand; Ore 1 [a] intact and [b] exposed mineralised surface; Ore 2 [c] intact and [d] exposed surface; Ore 3 [e] intact and [f] exposed surface; [g] Ore 3 treated at 0.4kWh/t.

http://dx.doi.org/10.1016/j.mineng.2017.05.003

The GRD index returned a significant beneficial change of between 4 and 13% for almost all of the tests across both campaigns. During Phase I, the change in percent passing 4.75mm was only significant for three out of the seven tests, but appeared to increase with increase dose for Ores 2 and 3 up to a maximum of approximately 16%. During Phase II, the percent passing 4.75mm was highly significant but fairly stable with increasing dose, with a change of typically 30-35%. Notably, the percent passing 4.75mm was two to three times higher in Phase II compared to Phase I. This suggests that exposing more ore to a region of high electric field strength (even with half the power density and one third of the total microwave treatment energy dose) has correlated with more observable microwave-induced fracture.

Table 3

Phase I JKGeM Ci test summary

Test ID	GRD		CRU		%-4.75mm		Beneficial Change (%)			Confidence Level (%)		
	Mean	σ	Mean	σ	Mean	σ	GRD	CRU	%-4.75mm	GRD	CRU	%-4.75mm
Ore 1												
UT1	0.541	0.003	2.42	0.23	11.3	0.8	-	-	-	-	-	-
T1	0.499	0.002	3.30	0.02	13.0	0.4	7.9	36.4	14.7	100	97	87
Ore 2												
UT1	0.601	0.013	3.05	0.17	11.6	0.1	-	-	-	-	-	-
T1	0.525	0.013	2.92	0.00	10.8	1.0	12.7	-4.3	-6.9	97	61	64
T2	0.542	0.004	3.24	0.10	12.9	0.3	9.8	6.2	11.4	98	70	97
T3	0.538	0.002	3.04	0.01	13.5	0.7	10.6	-0.5	16.6	98	9	95
Ore 3												
UT1	0.575	0.002	3.06	0.02	14.1	0.0	-	-	-	-	-	-
T1	0.518	0.004	2.55	0.07	13.4	0.6	9.8	-16.5	-4.3	100	99	74
T2	0.503	0.002	2.57	0.02	13.6	0.2	12.5	-16.0	-3.4	100	100	95
T3	0.505	0.012	2.53	0.08	14.1	0.1	12.2	-17.2	0.5	99	99	43

Table 4

Phase II JKGeM Ci test summary

Test ID	GRD		CRU		%-4.75mm		Beneficial Change (%)			Confidence Level (%)		
	Mean	σ	Mean	σ	Mean	σ	GRD	CRU	%-4.75mm	GRD	CRU	%-4.75mm
Ore 1												
UT2	0.493	0.006	2.94	0.17	11.8	0.7	-	-	-	-	-	-
T4	0.467	0.006	3.11	0.15	15.9	0.4	5.4	5.9	35.3	100	75	100
T5	0.470	0.010	3.14	0.10	15.7	0.5	4.7	6.9	33.5	98	85	100
T6	0.473	0.015	3.08	0.23	15.5	1.1	4.1	4.8	32.2	90	55	99
Ore 2												
UT2	0.577	0.017	2.99	0.13	11.9	0.4	-	-	-	-	-	-
T4	0.603	0.006	3.09	0.08	16.2	0.1	-4.6	3.3	36.7	94	69	100
T5	0.529	-	3.20	-	18.4	-	8.3	7.0	54.7	99	95	100
T6	0.545	0.039	3.00	0.16	16.2	0.6	5.4	0.3	36.4	73	6	100

Although the CRU index typically returned a beneficial change of up to 7% for Ores 1 and 2 during Phase II testing, the results were largely not significant. However, the CRU index returned a highly significant and apparently detrimental change to Ore 3 down to -17% during Phase I testing. This does not mean that microwave treatment has made the ore more competent, as the difference would conventionally suggest when comparing different ore types for geometallurgical purposes. Rather, induced fracturing around microwave-heating phase grain boundaries has altered the breakage behaviour during crushing, changing the breakage pattern and resulting particle size distribution. It is suggested that Ore 3 behaves differently from Ores 1 and 2 due to the coarser and more abundant sulphide mineralisation, perhaps affecting the coarser end of the crushing product size distribution more than the finer end. In other words, fine grained ores (such as Ore 1 and 2) may manifest breakage behaviour changes in the GRD index and percent passing 4.75mm, whereas coarse grained ores may manifest breakage behaviour changes in the GRD and CRU indices. The JKGeM Ci test product size distributions are provided in the Supplementary Information for reference. In either case, the JKGeM Ci test has demonstrated evidence of the prevalence of microwave-induced fractures in all three ore types.

http://dx.doi.org/10.1016/j.mineng.2017.05.003

Interestingly, there appeared to be little difference in outcome between T4 (0.7kWh/t) and T6 (1.5kWh/t) for either ore type, suggesting that doubling the energy and power density had no discernable impact on the prevalence of microwave-induced fracture. However, there was a noticeable difference between T1 (1.4kWh/t) and T3 (3.3kWh/t) treatments with increasing energy for Ores 2 and 3. This comparison suggests that homogeneity of treatment is more important than dose or power density as long the minimum dose and power density required for microwave-induced fracture is provided; in this case, less than or equal to approximately $3.3x10^6 W/m^3$ and 0.7kWh/t. Above this threshold, increasing the dose only serves to propagate microwave-induced fractures further leading to more macro-fracture in susceptible fragments but providing diminishing comminution benefit returns on a bulk ore basis. The apparent rate of diminishing return with increasing microwave treatment energy has also been frequently noted in batch laboratory experiments and numerical modelling work, and suggests an optimum cost-benefit trade off exists (Ali and Bradshaw, 2010; Batchelor et al., 2015; Jones et al., 2007; Kingman et al., 2004a; Kingman et al., 2004b; Whittles et al., 2003).

3.3 BBMWi test results

The BBMWi test was modified in these investigations. It was previously shown that the microwave-treated material typically yielded a finer crushing product size distribution compared to untreated material due to the impact of microwave-induced fractures, evidenced by a higher percent passing 4.75mm. To directly compare the work index of the untreated and microwave-treated material it was necessary to artificially alter the BBMWi test feed size distribution of the microwave-treated samples to be the same as the untreated material. In this way, the work index value may be used as a true comparison of any change in ore competency and not a function of different feed size distributions (e.g. for calculating relative or operating work index values). Each size class was carefully adjusted to have less than a 1% relative difference to the percent retained in the untreated control sample.

The details of the BBMWi tests are given in Table 5. Only the Ore 2-UT1 and Ore 2-T2 samples were tested during Phase I and the tests were performed in duplicate with a closing screen of 150µm. The results indicated there was a significant reduction in work index of 2.6%. Although this would typically be considered to be within the limit of experimental error in the laboratory, the careful and controlled preparation of the test samples, coupled with coefficients of variation (CoV, a.k.a. relative standard deviation) well below the industry standard of 3.4% (Bailey et al., 2009), lend the authors to believe the difference was indeed a function of microwave treatment.

Table 5

Phase I and Phase II BBMWi test summary

Test ID	F_{80} (µm)		P_{80} (µm)		Gbp (g/rev)		BBMWi (kWh/t)			Beneficial Change (%)	Confidence Level (%)
	Mean	σ	Mean	σ	Mean	σ	Mean	σ	CoV (%)		
Ore 1											
UT2	2061	16	161	0.6	3.393	0.098	9.27	0.21	2.3	-	-
T4	2038	3	162	0.6	3.445	0.047	9.19	0.08	0.9	0.9	44
T5	2057	24	161	0.6	3.501	0.030	9.03	0.06	0.7	2.5	86
T6	2047	3	162	0.6	3.421	0.016	9.23	0.02	0.3	0.4	24
Ore 2											
UT1	2108	11	113	0.0	1.716	0.003	13.76	0.03	0.2	-	-
T2	2121	25	113	0.0	1.770	0.006	13.41	0.06	0.4	2.6	98
UT2	2140	37	156	0.6	2.028	0.026	13.69	0.17	1.3	-	-
T4	2112	14	157	0.6	2.284	0.030	12.50	0.10	0.8	8.7	100
T5	2135	21	157	0.6	2.181	0.041	13.00	0.21	1.6	5.0	99
T6	2134	17	158	1.0	2.255	0.025	12.69	0.11	0.8	7.3	100

During Phase II, the tests were performed in triplicate on all samples with a closing screen of 212µm. Ore 2 yielded highly significant results with a reduction in BBMWi of approximately 5-9%, a two to three fold increase of what was observed during Phase I. This further supports the previous suggestion that exposing more ore to a region of high electric field strength (even with half the power density and one third of the total microwave treatment energy dose) has correlated with more microwave-induced fracture. The Ore 1 samples did not yield a significant result, with the changes in work index less than 2.5%. Therefore, it would appear that the microwave-induced fractures have been largely exhausted during the crushing stages. A wide range of microwave treatment energies were not investigated as part of the Phase II testing campaign. However, historical low power density batch microwave treatments have also demonstrated an apparent rate of diminishing return with increasing dose for the BBMWi test on a variety of ore types (Kingman et al., 2000a, b).

http://dx.doi.org/10.1016/j.mineng.2017.05.003

3.4 JKDW test results

The JKDW test was not performed during the Phase I campaign. The A*b values used in the Phase I flowsheet modelling for the untreated samples (denoted as UT) were taken from previous work done on the same ores found in the JKTech database. The A*b values for the microwave-treated material (denoted as T) were estimated to be 7% larger based on previous unpublished work, and which was subsequently justified by the results from Phase II testing. These figures and the results of the full and modified JKDW tests conducted as part of Phase II are given inTable 6.

Table 6

Phase II JKDW test A*b values and assumed Phase I A*b values

Test ID	Modified JKDW	Full JKDW	Calculated JKDW	
			A*b	Change (%)
Ore 1				
UT	-	56.3	56.3	-
T	-	-	60.2	7
UT2	43.0	44.9	44.9	-
T4	46.7	N/A	48.1	7
T5	40.1	N/A	41.3	-8
T6	40.3	N/A	41.5	-8
Ore 2				
UT	-	36.6	36.6	-
T	-	-	39.2	7
UT2	45.8	39.3	39.3	-
T4	46.2	N/A	39.6	1
T5	45.8	N/A	39.3	0
T6	52.2	N/A	44.8	14
Ore 3				
UT	-	73.8	73.8	-
T	-	-	79.0	7

It can be seen that only the Ore 1-T4 and Ore 2-T6 treatments demonstrated an apparent improvement in A*b. The Ore 1-T4 treatment produced a 7% softening of the ore, which was inline with that estimated for the Phase I samples. However, it appears from the Ore 1-T5 and Ore 1-T6 samples that the margin of error for the test is approximately ±8%, which is supported by a similar study by Rizmanoski (2011). The Ore 2-T6 sample exceeds this margin of error, yielding a 14% softening of the ore, but with Ore 2-T4 and Ore 2-T5 showing no difference. It is likely that a higher microwave treatment energy was required to provide a measurable difference in the Ore 2 ore type, as was found by other researchers with other ores where up to 40% changes in A*b were noted at higher microwave treatment energy doses (Kingman et al., 2004b; Rizmanoski, 2011).

The JKGeM Ci and BBMWi test results indicated that all three microwave treatments for both ores introduced measurable microwave-induced fractures, but these are apparently largely unmeasurable by the JKDW test. One reason may be that the test preferentially exploits only the most extensive microwave-induced macro-fractures. The nature of the fixed energy single breakage event mechanism may mask the presence of micro-fractures which can be exploited by the JKGeM Ci test or BBMWi test. It may also have been that the JKDW test energy levels were too high to observe any differences in the Ore 1 samples and lower microwave treatment energy Ore 2 samples (Kingman et al., 2004b; Rizmanoski, 2011). However, low energy drop weight tests would typically be below that expected in real world applications. In contrast, the Point Load Index test employed in early investigations measures the minimum force required for breakage, which potentially provides a higher level of sensitivity. However, the A*b values are essential to flow sheet modelling and so the standard JKDW test energies are required unless a correlation with another metric can be provided within a suitable accuracy.

http://dx.doi.org/10.1016/j.mineng.2017.05.003

Another reason may potentially be a sample size issue in that the JKDW test does not require many fragments to be used for the standard test protocol. Visual observation of the ores post-microwave treatment demonstrated that as little as approximately 5% of the fragments contained varying degrees of visible macro-fracture. The heterogenous nature of the ores means there are also many fragments that are effectively microwave-heating phase barren or may have a soft matrix and not be susceptible to microwave-induced fracturing (Batchelor et al., 2015). So the test may essentially rely on one heavily damaged fragment out of 20 being selected in the test sample. Any future analysis should therefore consider the full JKDW test and significantly increasing the sample mass for each size class tested to ensure every degree of microwave-induced fracture and mineralogical texture is captured representatively in the test samples.

4 Liberation analysis

4.1 Phase I testing

The liberation charts for combined size classes of the Phase I treatments on Ores 1, 2 and 3 are given in Figure 5, Figure 6 and Figure 7 respectively. Ore 1 shows only a slight improvement (1.4%) in the highly liberated (>98%) material for the coarse grind at P_{80} 350µm; however there was a marked increase (6%) in the highly liberated material for the fine grind at P_{80} 150µm for the lower energy T1 treatment. In contrast, there also appears to be an increase in the <90% liberation classes for the fine grind. It appears that preferential breakage around copper sulphide grains due to microwave treatment has lead to the creation of more highly liberated grains but left behind more locked mineral due to incomplete release of the grains.

Ore 2 also showed only slight changes in the liberation profiles for coarse grinds in the range P_{80} 350-600µm. However, there was a marked increase (4.7-8.2%) in the highly liberated material for the finer P_{80} 150µm grinds increasing with microwave treatment energy dose. The amount of lower grade middlings (<90%) also reduced with increasing treatment energy dose after a notable rise for the lower energy T1 treatment.

Similar to both Ores 1 and 2, Ore 3 showed little difference in liberation profile for the coarse grinds. However there was a 6.3-8.3% increase in the amount of highly liberated mineral following microwave treatment, with the same incomplete release phenomena noted with the Ore 1 sample leading to a higher proportion of <90% liberation class material.

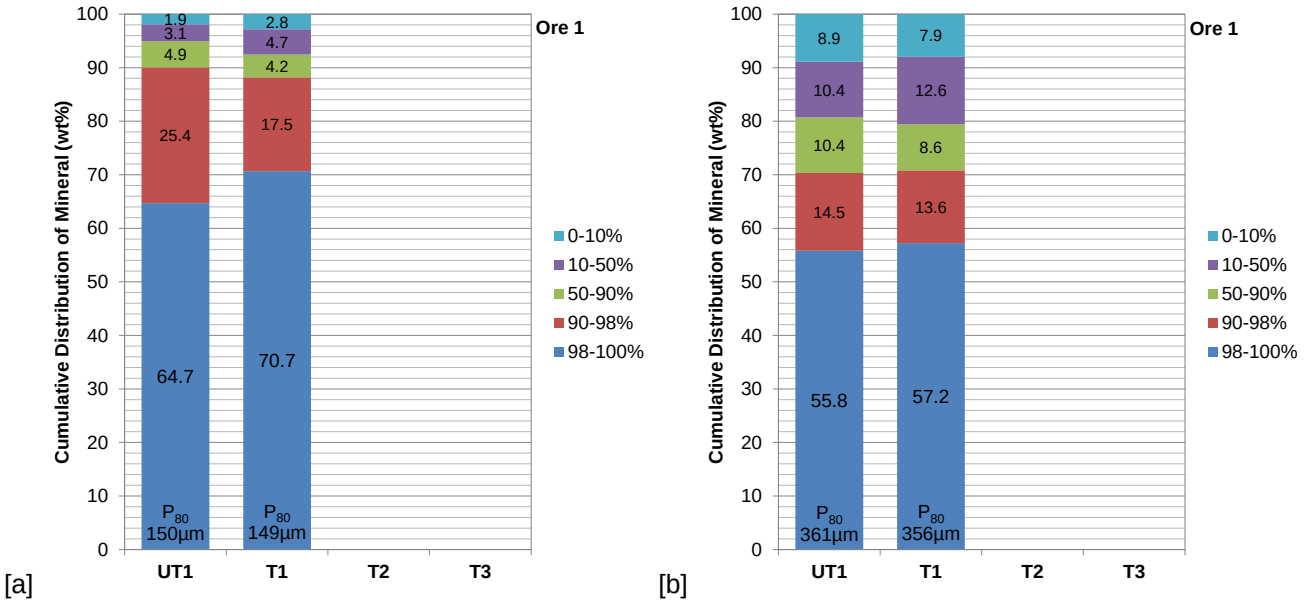

Figure 5: Phase I Ore 1 copper sulphide liberation for the [a] P_{80} 150µm and [b] P_{80} 350µm grinds

http://dx.doi.org/10.1016/j.mineng.2017.05.003

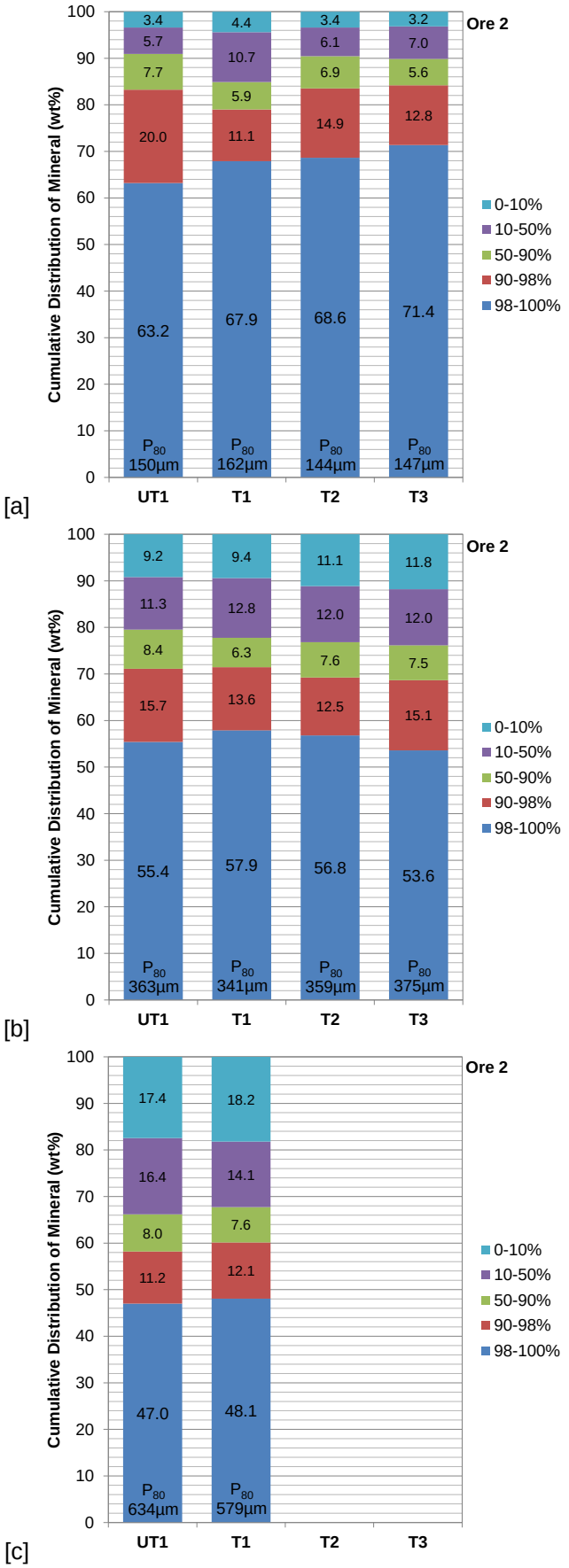

Figure 6: Phase I Ore 2 copper sulphide liberation for the [a] P_{80} 150µm, [b] P_{80} 350µm and [c] P_{80} 600µm grinds

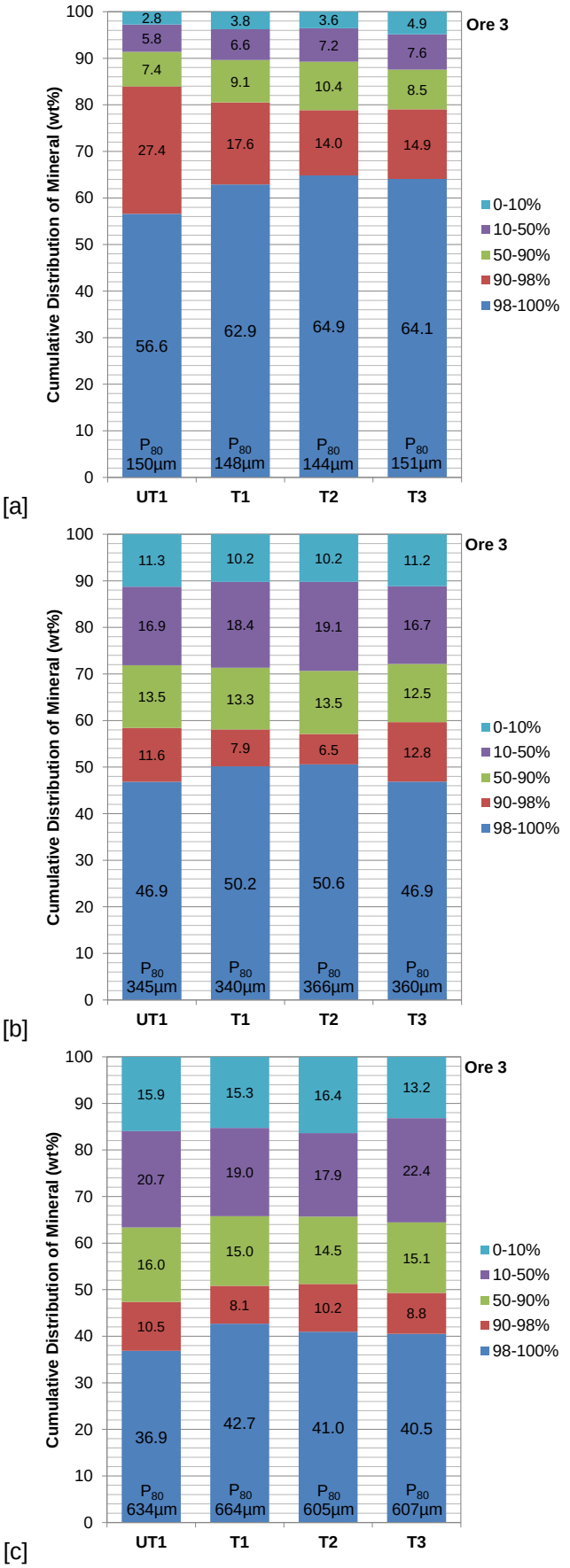

Figure 7: Phase I Ore 3 copper sulphide liberation for the [a] P_{80} 150µm, [b] P_{80} 350µm and [c] P_{80} 600µm grinds

http://dx.doi.org/10.1016/j.mineng.2017.05.003

4.2 Phase II testing

The dual applicator Phase II treatment liberation charts are presented in Figure 8 and Figure 9 for Ores 1 and 2 respectively. Despite microwave treatments being performed at lower total microwave treatment energy doses than Phase I (with single applicator doses ranging from 0.3 to 0.7kWh/t), both ores now demonstrated improved liberation at the coarser grind sizes around P_{80} 400µm. This is believed to be due to more ore passing through a region of higher electric field strength leading to more homogeneous and effective treatment.

Ore 1 now demonstrates a 2.9-6.7% increase in the highly liberated fraction following microwave treatment even though the T4 and T6 treatment liberation grinds are 55-65µm coarser than the untreated coarse grind. The incomplete release phenomena also occured 200-300µm coarser than observed during Phase I. The increase in the amount of highly liberated material increases to 6.6-10.2% at the finer grinds and this has translated into a higher proportion of >60% liberated material compared to the untreated sample.

Similarly, Ore 2 exhibits a 3.9-4.1% increase in the amount of the highly liberated material for the coarse grinds where the T4 and T6 treatments are 35-80µm coarser than the untreated sample. There is also a decrease in the amount of <60% and <30% liberated material that becomes more pronounced at the fine grinds. The amount of highly liberated material also increases to 10.4-11.7% at the fine grinds.

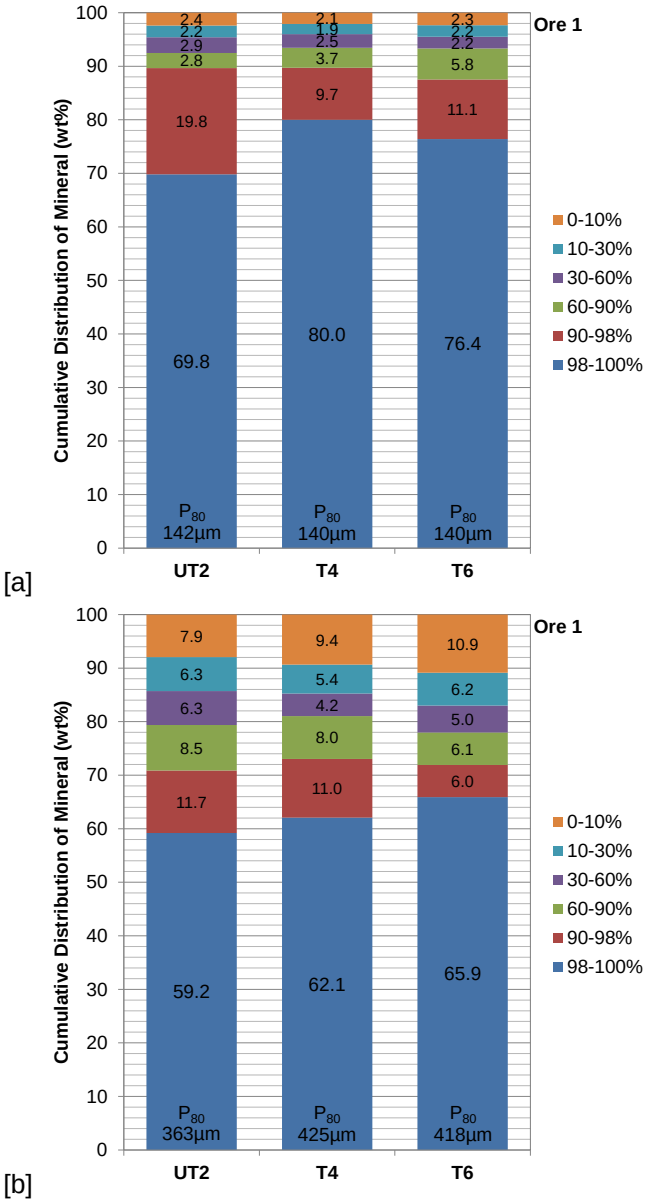

Figure 8: Phase II Ore 1 copper sulphide liberation for the [a] P_{80} 150µm and [b] P_{80} 350/425µm grinds

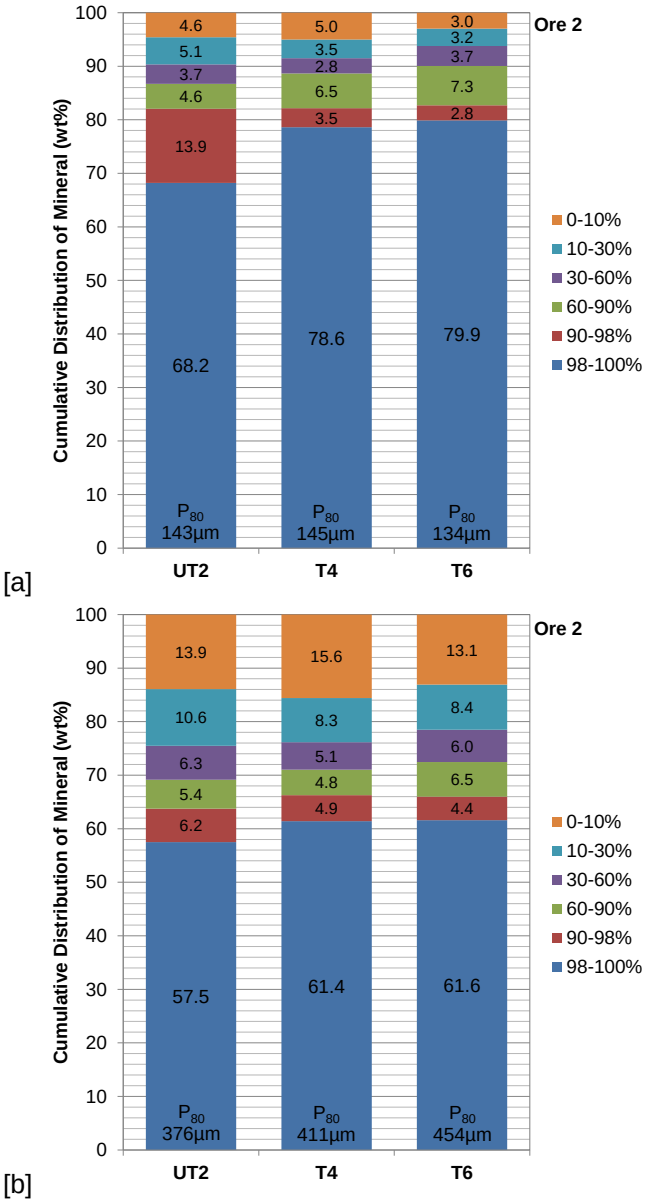

Figure 9: Phase II Ore 2 copper sulphide liberation for the [a] P_{80} 150µm and [b] P_{80} 350/425µm grinds

http://dx.doi.org/10.1016/j.mineng.2017.05.003

While the highly liberated fractions are perhaps most important for flotation, locking behaviour of the middlings will also be important to copper recovery. The change in locking behaviour of the copper sulphides with pyrite and non-sulphide gangue at the different grind sizes is given in Figure 10 and Figure 11 for Ore 1 and 2 respectively. Both ore types demonstrated that the increase in copper sulphide liberation following microwave treatment corresponded to a decrease in binary particles with non-sulphide gangue. The changes in binary particles with pyrite were typically within ±1% and no consistent trends were apparent. There was also little change in the ternary particles.

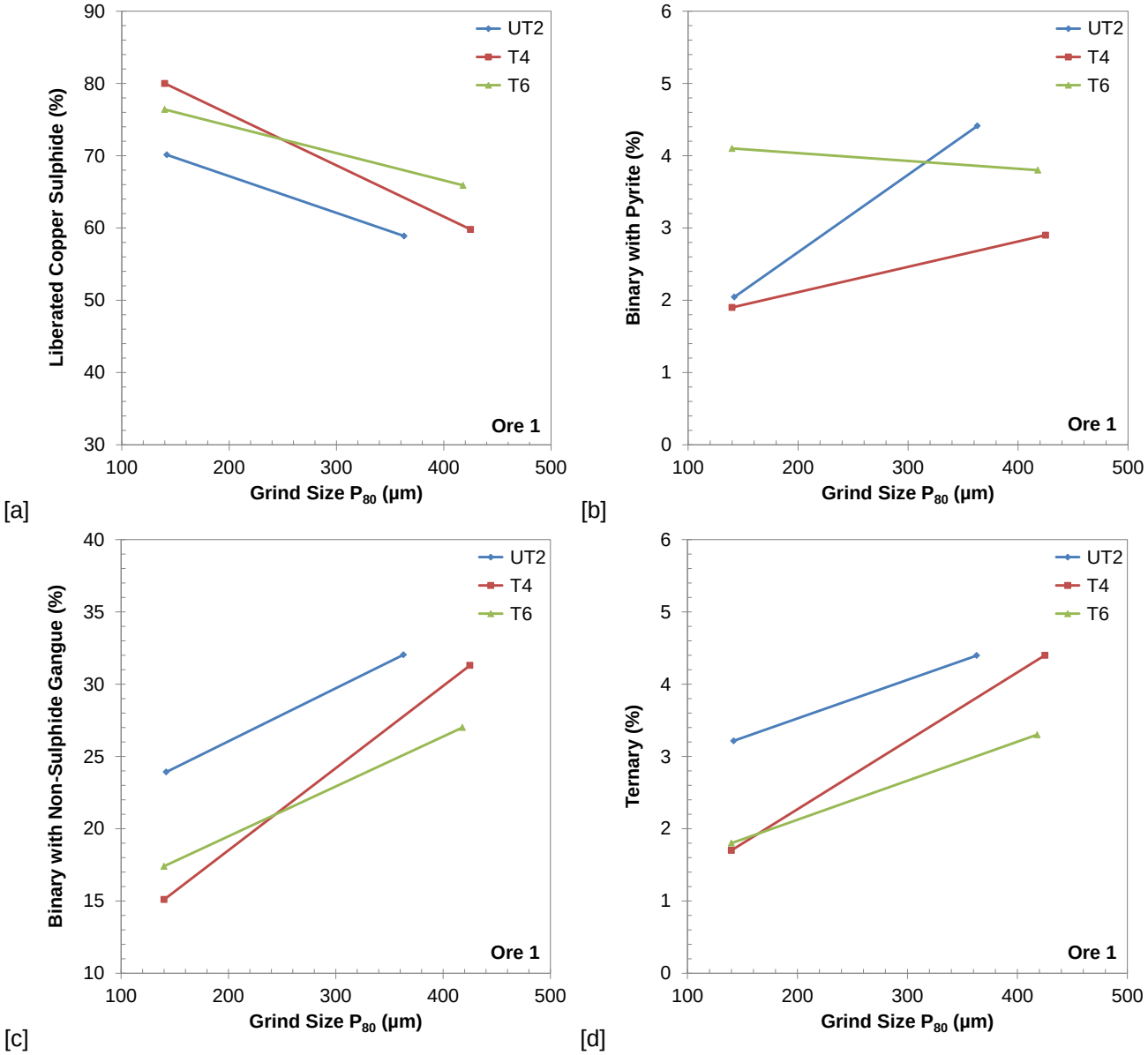

Figure 10: Phase II Ore 1 copper sulphide locking data (5% tolerance) [a] liberated, [b] binary with pyrite, [c] binary with non-sulphide gangue, and [d] ternary

The change in locking behaviour of pyrite for Ore 2 followed the same trends as the copper sulphides, with an increase in liberated pyrite following microwave treatment corresponding to a decrease in binary particles with non-sulphide gangue. In contrast, the locking behaviour of pyrite in Ore 1 appeared to follow a different trend. There was an apparent decrease in the amount of liberated pyrite at the fine grinds following microwave treatment corresponding to an increase in binary particles with copper sulphides. Ore 1 had a significant proportion of pyrite locked in binary particles with copper sulphides and it appears that preferential breakage following microwave treatment has occurred around bulk sulphide grains leading to incomplete release of the pyrite from copper sulphides. The pyrite locking charts are given in Figure S.3 and Figure S.4 for Ore 1 and 2 respectively in the Supplementary Information.

http://dx.doi.org/10.1016/j.mineng.2017.05.003

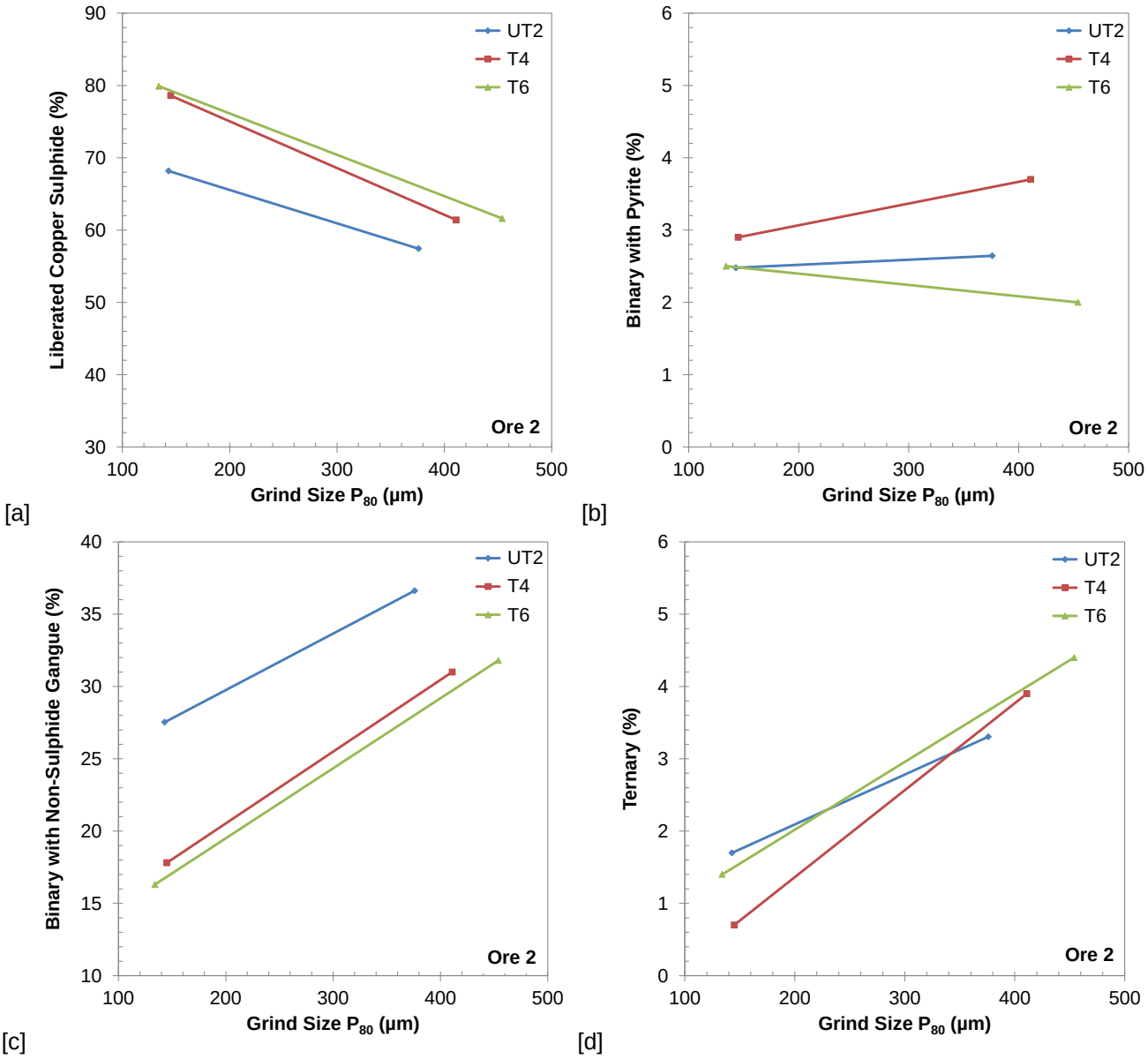

Figure 11: Phase II Ore 2 copper sulphide locking data (5% tolerance) [a] liberated, [b] binary with pyrite, [c] binary with non-sulphide gangue, and [d] ternary

Given that the changes in liberation appear to occur around the 60% liberation class and that >60% liberated material would have superior flotation performance to the <60% liberated material, the proportion of copper sulphide >60% liberated was plotted against grind size, shown in Figure 12. It can be seen that at the nominal plant grind size of P_{80} 190µm there is an estimated increase of 1-1.5% of liberated (>60%) material for Ore 1 and 2.5-4% for Ore 2. At a fixed proportion of liberated (>60%) material corresponding the untreated samples at P_{80} 190µm, there is an estimated 20-40µm increase in P_{80} for Ore 1 and 40-70µm increase in P_{80} for Ore 2 for equivalent liberation following microwave treatment.

http://dx.doi.org/10.1016/j.mineng.2017.05.003

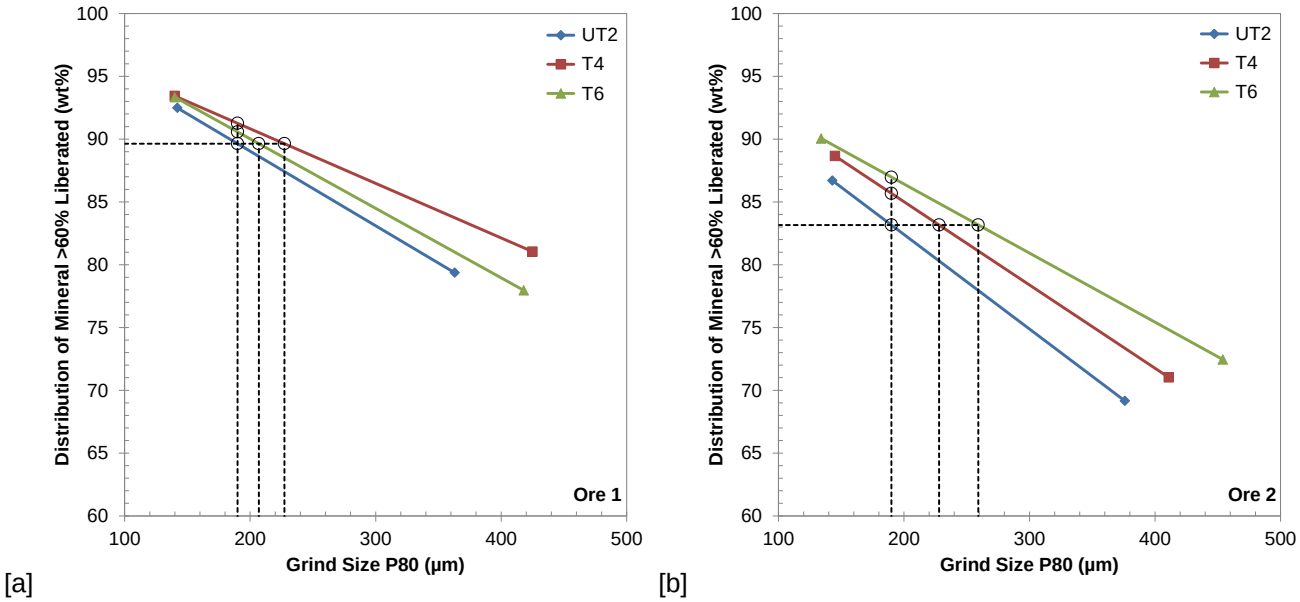

Figure 12: Phase II copper sulphide liberation by grind size for [a] Ore 1 and [b] Ore 2

5 Discussion

5.1 Comminution and liberation results

The more marginal liberation improvements for Ore 1 appear to correlate with the less pronounced comminution benefits and perhaps also because Ore 1 is more highly liberated than Ore 2 overall at the grind sizes tested. Ore 2 had an approximate four-fold higher pyrite content than Ore 1, which would likely have aided in microwave-induced fracture of the ore and inter-granular breakage around associated copper sulphide grains due to the different elastic properties of chalcopyrite and pyrite minerals compared to the matrix (Batchelor et al., 2016; Djordjevic, 2014), despite being partly constrained by a softer matrix containing a significant proportion of mica, which has been shown to limit comminution benefits (Ali and Bradshaw, 2009; Batchelor et al., 2015; Kingman et al., 2000b).

The pilot scale liberation results are in good agreement with small batch laboratory experiments performed on a different porphyry copper ore investigated by Batchelor et al. (2016). In that study, the ore was treated at 15kW in a single mode applicator with approximately 2kWh/t total energy input provided by two passes of 1kWh/t each, mimicking the dual applicator configuration adopted in the pilot scale test facility. It was shown that grind size could be increased by 50-60µm to achieve equivalent liberation and milling Work Index was also shown to be reduced by 4-8% compared to the untreated control sample. The copper and iron sulphides were highly associated with each other in this ore and notable changes in copper and iron sulphide association were observed following microwave treatment and batch grinding. In comparison, given the relatively small amount of binary particles with pyrite (<5%) and that the textural analysis indicated that copper and iron sulphides were not highly associated with one another for Ore 1 and 2 in this investigation, it is perhaps not surprising there was little change noted in copper and iron sulphide locking behaviour for these two ore types.

In contrast, the more dramatic improvements in comminution, liberation and flotation performance reported with small batch laboratory experiments on a copper carbonatite ore, containing a significant proportion of magnetite and coarse sulphide mineralisation, under similar microwave treatment conditions (Kingman et al., 2004b; Sahyoun et al., 2005; Scott et al., 2008) are more likely related to mineralogical and thermo-mechanical properties, highlighting that some ore types are more susceptible to microwave treatment than others (Ali and Bradshaw, 2009, 2010; Batchelor et al., 2015; Kingman et al., 2000b).

http://dx.doi.org/10.1016/j.mineng.2017.05.003

5.2 Future considerations for industrial scale microwave treatment of ores

During pilot testing, the ore/fines blend used a high proportion of fines to enable mass flow of the coarsest fragments possible through a relatively narrow tube. By scaling up to the next frequency (i.e. reducing frequency from 896/915/922MHz to 350/433MHz) and/or designing larger diameter multimode applicators it should be possible to achieve higher throughputs (>>150t/h in a single treatment module) with particle size distributions akin to common SAG mill feed distributions. Microwave treatment investigations on >50mm size fragments would be very beneficial in that it would help account for a larger proportion of typical ROM feed size distributions and help determine any potential effective reduction in F_{80}, which has a large impact on circuit performance. The ability to handle wider size distributions would further serve to mitigate expenditure on any additional crushing and screening steps prior to microwave treatment. However, it has also been demonstrated that any new applicator should be designed to support a more homogeneous electric field distribution with at least the minimum required beneficial peak power density accounting for the majority of the applicator cross-sectional area. This would allow the maximum benefit to be achieved at the lowest possible microwave treatment energy dose.

Further consideration must also be given to the selection of materials for the applicator treatment tube. The quartz and ultra high molecular weight polyethylene (UHMW-PE) tube sections were only chosen for use in the batch wise operation of the pilot plant to minimise cost (as they were available off-the-shelf and/or cheap to produce) and enable visualisation of the load. A more robust, hard wearing and thermally stable ceramic with similarly low dielectric properties would likely be required as an industrial solution. Although the thin quartz tube was quite fragile and did break at times following a long duty cycle requiring a changeout, the use of a fine primer and loading protocols ensured that damage was limited during the most vulnerable stage of the process. Little scoring of the quartz was noted due to the detailed design for stress minimisation in the applicator, discussed in detail in the first part of this paper (Buttress et al., 2017).

5.3 Comminution circuit modelling

There are several possible metallurgical benefits of microwave-induced fracture that may be exploited including enhanced liberation and increased values recovery, with increased grind size and reduced comminution energy consumption that may also lead to increased throughput. Although these investigations have focussed on the potential for increased grind size for equivalent liberation, different mines, and indeed different ore types, may benefit more from one than another. It is therefore useful to demonstrate the potential value of an industrial scale microwave treatment system by considering the impact of the potential benefits on comminution circuit performance through circuit modelling exercises.

The host mine comminution circuit comprised a SAG mill closed by a trommel screen and recycled pebble crusher feeding two ball mills in parallel closed by hydrocyclones (SABC circuit). The circuit throughput is limited by the SAG mill. A JKSimMet model of the host mine circuit, illustrated in Figure 13, was used in the Phase I circuit modelling exercise.

Major throughput gains could not be realised across the SAG mill limited circuit without making significant changes to SAG mill operating parameters. As a result, during Phase I modelling, changes to the SAG circuit operating conditions were modelled to increase the transfer size (T_{80}) from the SAG circuit to the ball mill circuit and consequently increase SAG throughput. The equipment specifications and other operating conditions were maintained at the host mine operating values except for the cyclone vortex finder, which was altered to maintain the ball mill circuit circulating load close to the base case. The final product size was monitored to ensure that it didn't exceed the flotation feed size requirements.

Ore properties contained in the JKTech database were used for the base case model where no standard comminution tests were performed during the Phase I campaign. JKDW test A*b values were estimated for the microwave treated samples as mentioned previously and it was assumed there was no improvement in BBMWi. The SAG mill F_{80} was lowered by 30% for the microwave-treated samples to account for finer crushing product size distributions and a faster initial rate of breakage for heavily fractured fragments, assuming that a coarser feed was microwave-treated prior to crushing for SAG mill feed. The modelling exercise varied operating conditions and ore properties independently, and then together to assess the impact on ball mill P_{80}, throughput and specific comminution energy (E_{CS}). The pertinent model inputs and outputs are given in Table 7 and Figure 14.

It can be seen that the change in ore properties from microwave treatment had a larger independent beneficial impact on throughput (up to 22% increase) and specific comminution energy (up to 18% reduction) than altering the operating conditions (up to 8% increase in throughput and 7% reduction in specific comminution energy), with similar resultant ball mill P_{80} sizes. By changing both together, a throughput increase of up to 29% and reduction in specific comminution energy of 22% was obtained with a resultant 30µm coarser ball mill P_{80} size. The 30µm increase in grind size was within the range that suggested equivalent liberation between microwave-treated and

http://dx.doi.org/10.1016/j.mineng.2017.05.003

untreated material. A higher transfer size yielded a 23% increase in throughput, 54µm coarser grind size and 18% reduction in specific comminution energy.

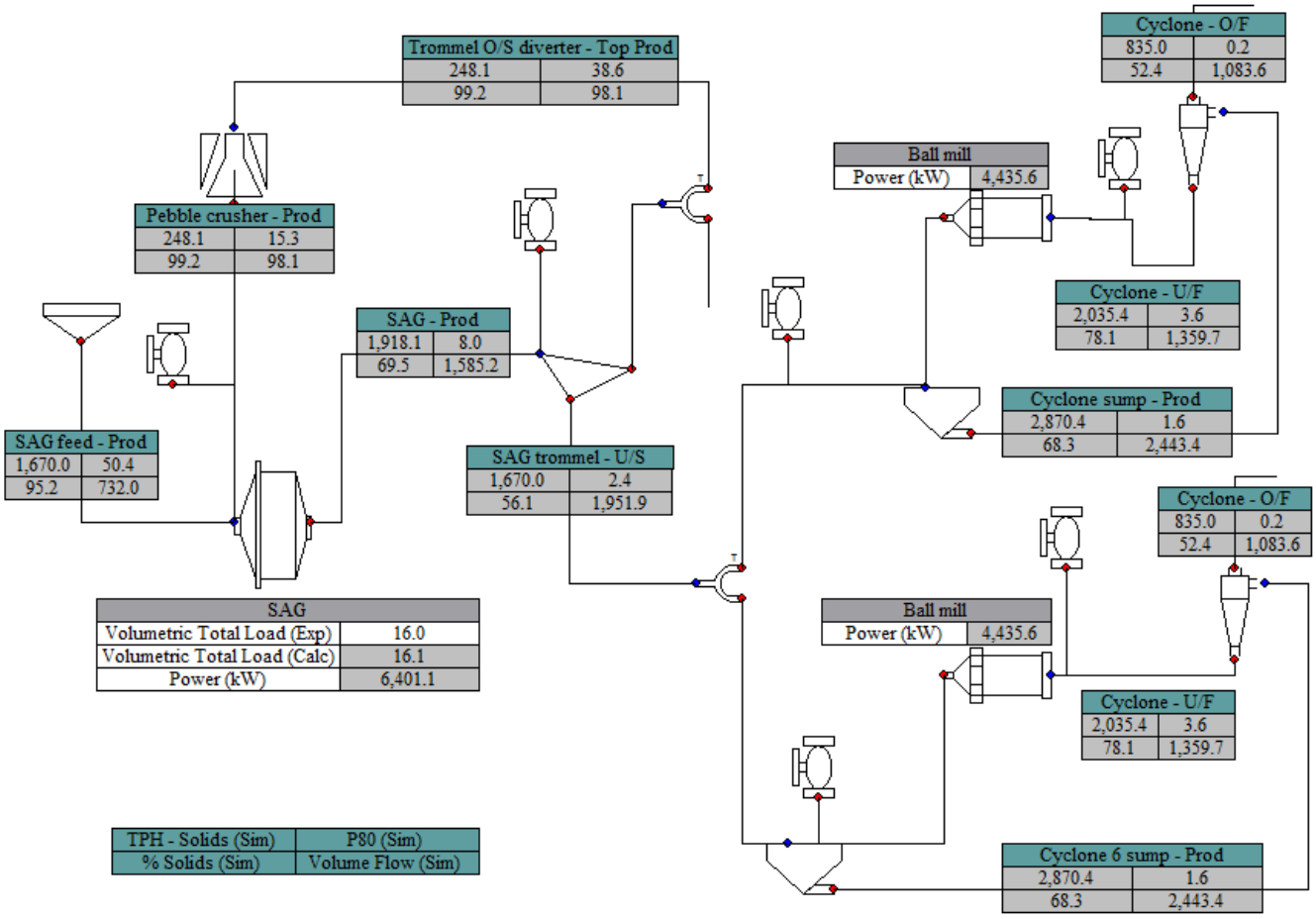

Figure 13: Schematic diagram of the constrained host mine circuit

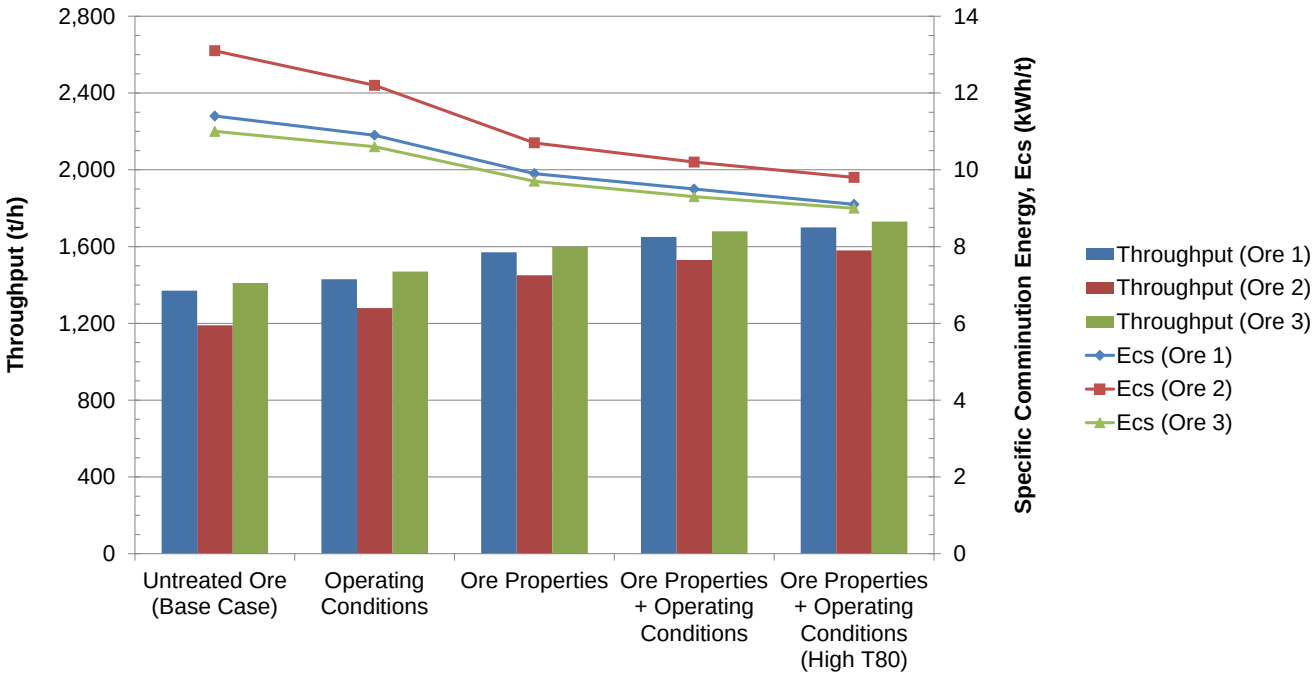

Figure 14: Phase I flow sheet modelling outputs constrained to host mine circuit

http://dx.doi.org/10.1016/j.mineng.2017.05.003

Table 7

Phase I flowsheet modelling

Operating Conditions & Ore Properties	Base Case	Simulated Changes			
	Untreate Ore	Operating Conditions	Ore Properties	Ore Properties & Operating Conditions	Ore Properties & Operating Conditions (High T_{80})
Ore 1					
Inputs					
SAG Pebble Port (mm)	62	76	62	76	76
Trommel Aperture (mm)	10	15	10	15	22
Cyclone Vortex Finder (mm)	254	300	254	300	300
F_{80} (mm)	50.4	50.4	35.3	35.3	35.3
A*b	56.3	56.3	60.2	60.2	60.2
BBMWi (kWh/t)	9.9	9.9	9.9	9.9	9.9
Outputs					
P_{80} (µm)	190	206	210	226	248
Throughput Change (%)	-	4	15	20	24
E_{CS} Change (%)	-	-4	-13	-17	-20
Ore 2					
Inputs					
SAG Pebble Port (mm)	62	76	62	76	76
Trommel Aperture (mm)	10	15	10	15	22
Cyclone Vortex Finder (mm)	300	300	300	330	380
F_{80} (mm)	50.4	50.4	35.3	35.3	35.3
A*b	36.6	36.6	39.2	39.2	39.2
BBMWi (kWh/t)	12.6	12.6	12.6	12.6	12.6
Outputs					
P_{80} (µm)	204	225	229	252	294
Throughput Change (%)	-	8	22	29	33
E_{CS} Change (%)	-	-7	-18	-22	-25
Ore 3					
Inputs					
SAG Pebble Port (mm)	62	76	62	76	76
Trommel Aperture (mm)	10	15	10	15	22
Cyclone Vortex Finder (mm)	254	300	254	300	330
F_{80} (mm)	50.4	50.4	35.3	35.3	35.3
A*b	73.8	73.8	79.0	79.0	79.0
BBMWi (kWh/t)	8.7	8.7	8.7	8.7	8.7
Outputs					
P_{80} (µm)	197	208	212	227	251
Throughput Change (%)	-	4	13	19	23
E_{CS} Change (%)	-	-4	-12	-15	-18

In order to fully explore the impact of microwave treatment on the comminution circuit throughput, two SABC flowsheets, namely a constrained circuit and an unconstrained circuit, were used in the Phase II modelling exercise. The Constrained flow sheet was the same base case used in Phase I modelling, given in Figure 13, with adjustments to only the ball mill load fraction and cyclone parameters to ensure the target P_{80} was achieved. The Unconstrained flow sheet utilised equipment specifications and operating conditions designed to yield 1,600t/h at a P_{80} of 190µm with a SAG recycle rate of 20-25% and ball mill circuit circulating load of 250%, illustrated in Figure 15. During Phase II, standard comminution tests were performed to obtain real values for A*b and BBMWi, and the ball mill P_{80} fixed to either 190µm (nominal plant target grind size) or 290µm (maximum increase of 100µm for equivalent liberation).

http://dx.doi.org/10.1016/j.mineng.2017.05.003

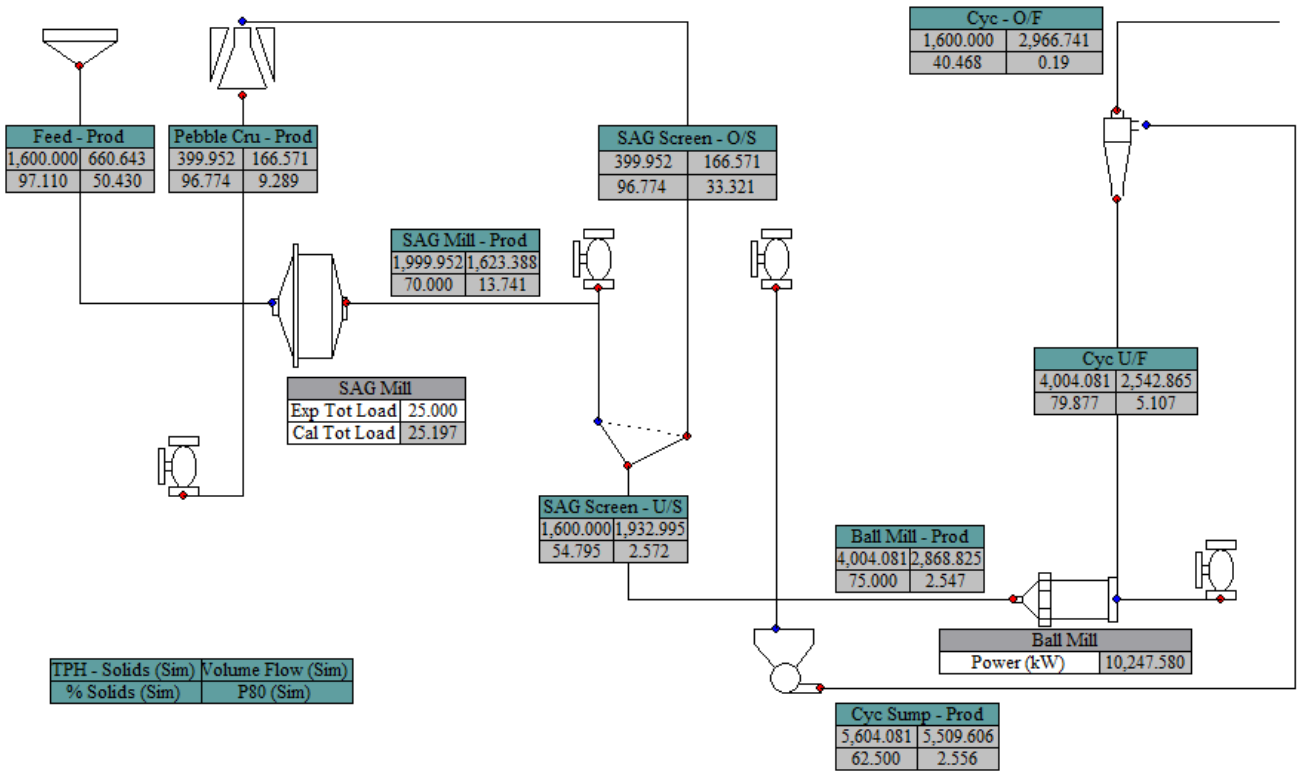

Figure 15: Schematic diagram of the unconstrained SABC circuit

Unlike in Phase I, the F_{80} was kept constant at a value consistent with the host mine operations for all the Phase II Constrained model simulations. The F_{80} for the Unconstrained model simulations was however increased to more typical industry values for the base case (~100mm). The F_{80} values used were derived using a methodology that relates the primary crusher, close side setting (CSS) and ore hardness (Drop-Weight Index, DWi) to the primary crusher product P_{80} (Bailey et al., 2009). This methodology accounts for the different resistances of the ore to impact breakage in the primary crushing stage. The primary crusher product P_{80} size (i.e. the SAG mill feed F_{80}) therefore expresses the changes in the ore hardness. The microwave-treated F_{80} values were subsequently reduced by a small margin based on the reduction in ore competency from JKDW testing.

The pertinent model inputs and outputs are given in Table 8. It can be seen that for both ore types the Unconstrained circuit was simulated to realise more value from the microwave-treatment than the host mine constrained circuit, particularly for coarser grind sizes, demonstrating a wider applicability in Greenfield or similar Brownfield mine sites. At the nominal plant target grind size of 190µm, a throughput increase of up to 6% was simulated for the Constrained scenario and 10% for the Unconstrained scenario following microwave treatment, with reductions in E_{CS} of 5-9% depending on ore type. At 290µm, throughput increases of up to 18% for the Constrained and 28% for the Unconstrained scenarios (relative to the 190µm base case) were simulated, with reductions in E_{CS} of up to 18% and 24% respectively. A third grind size with a P_{80} of 425µm was also simulated but indicated negligible improvement above 290µm due to the limitations of the circuit.

It should be noted that reported specific comminution energy was for the milling circuit only and did not include the microwave treatment energy. Incorporating a microwave treatment energy dose of 0.7kWh/t resulted in a 2% increase to 4% reduction in net E_{CS} for nominal plant target grind size scenarios with a throughput increase of 0-10%. Under these circumstances the value proposition would likely be increased metal recovery, due to an improvement in liberation at the same grind size, coupled with the marginal throughput increase. Comminution energy savings and higher throughputs would be the value propositions via coarser grinding for the same metal recovery, with liberation equivalent to the nominal plant grind (assuming flotation was largely unaffected by grind size over a narrow grind size increase). Incorporating a 0.7kWh/t microwave dose resulted in a reduction in net E_{CS} of up to 6-19% with up to 16-33% higher throughputs for the coarse grind scenarios.

http://dx.doi.org/10.1016/j.mineng.2017.05.003

Table 8

Phase II flowsheet modelling

Operating Conditions & Ore Properties	Constrained to Host Mine Circuit				Unconstrained SABC Circuit			
	P_{80} 190µm		P_{80} 290µm		P_{80} 190µm		P_{80} 290µm	
	Untreated (Base Case)	Treated	Untreated	Treated	Untreated (Base Case)	Treated	Untreated	Treated
Ore 1								
Inputs								
F_{80} (mm)	50.4	50.4	50.4	50.4	102	98	102	98
A*b	44.9	48.1	44.9	48.1	44.9	48.1	44.9	48.1
BBMWi (kWh/t)	9.27	9.19	9.27	9.19	9.27	9.19	9.27	9.19
Outputs								
Throughput (t/h)	1,702	1,700	1,850	1,970	1,600	1,680	1,920	2,050
Throughput Change (%)	-	-0.1	8.7	15.7	-	5.0	20.0	28.1
E_{CS} (kWh/t)	9.4	8.7	8.2	7.7	13.6	12.9	11.2	10.7
E_{CS} Change (%)	-	-8.1	-12.6	-18.1	-	-4.9	-17.4	-21.2
Energy Balance								
Microwave Energy Dose (kWh/t)	0.0	0.7	0.0	0.7	0.0	0.7	0.0	0.7
Net Energy Input (kWh/t)	9.4	9.4	8.2	8.4	13.6	13.6	11.2	11.4
Net Energy Change (%)	-	0.0	-12.6	-10.6	-	0.3	-17.4	-16.1
Ore 2								
Inputs								
F_{80} (mm)	50.4	50.4	50.4	50.4	112	102	112	102
A*b	39.3	44.8	39.3	44.8	39.3	44.8	39.3	44.8
BBMWi (kWh/t)	13.69	12.69	13.69	12.69	13.69	12.69	13.69	12.69
Outputs								
Throughput (t/h)	1,500	1,590	1,728	1,756	1,600	1,764	1,868	2,130
Throughput Change (%)	-	6.0	15.2	17.1	-	10.3	16.8	33.1
E_{CS} (kWh/t)	9.6	9.1	8.5	8.3	15.5	14.1	13.7	11.8
E_{CS} Change (%)	-	-5.4	-11.1	-13.2	-	-8.8	-11.7	-23.6
Energy Balance								
Microwave Energy Dose (kWh/t)	0.0	0.7	0.0	0.7	0.0	0.7	0.0	0.7
Net Energy Input (kWh/t)	9.6	9.8	8.5	9.0	15.5	14.8	13.7	12.5
Net Energy Change (%)	-	2.1	-11.1	-6.3	-	-4.2	-11.7	-19.0

6 Conclusions and Recommendations

6.1 Summary of testing

A pilot scale microwave treatment system capable of treating 10-150t/h of material at 10-200kW yielding a microwave treatment energy dose range of 0.1-20kWh/t was designed, constructed and commissioned in a laborated-based environment in order to understand the engineering challenges of microwave-induced fracture of ores at scale. The pilot plant was subsequently used to generate large samples (in the order of 500kg) to determine the influence of dose, power density and treatment homogeneity on comminution and liberation performance for low dose (0.3-3kWh/t) microwave treatments on three different ore types.

It was demonstrated that exposing more of the ore to a region of high power density by improving treatment homogeneity with two applicators in series yielded equivalent or better metallurgical performance with up to half the power and one third the energy requirement of that used with a single applicator. Conventional comminution testing indicated that A*b values may be reduced by up to 7-14% and that BBMWi may be reduced by up to 3-9% depending on the ore type under investigation. JKGeM Ci testing also demonstrated that microwave-treated ores yield different breakage behaviour during crushing, typically resulting in a finer product size distribution. Liberation analysis of microwave-treated ore indicated that equivalent liberation may be achievable for a grind size approximately 40-70µm coarser than untreated ore, which is in agreement with laboratory scale investigations reported in the literature at similar or higher doses (Batchelor et al., 2016). Flow sheet simulations further indicated that reduced ore competency following microwave treatment could potentially yield up to a 9% reduction in specific comminution energy (E_{CS}) at a

http://dx.doi.org/10.1016/j.mineng.2017.05.003

nominal plant grind of P_{80} 190µm, or up to 24% reduction at a grind of P_{80} 290µm, for a microwave energy input of 0.7-1.3kWh/t. Throughput could also be increased by up to approximately 30% depending on grind size and ore type.

To date, approximately 300t of material has been processed through the pilot plant under microwave irradiation. Metallurgical testing has demonstrated that comminution and liberation benefits are achievable at doses lower than that previously reported in the literature, which allow high throughputs to be sustained with low installed power requirements. However, it has also been demonstrated that reducing dose and power density to maximise throughput may result in reduced benefits and that the efficiency of microwave-induced fracture is also dependent on the lithology and texture of the ore under examination.

6.2 Recommendations for future work

These most recent investigations have only considered three different porphyry copper ore types from the same mine in detail. It would be prudent to investigate a larger variety of ores and commodities to determine the wider applicability of the technology and to see if the large changes in comminution and liberation behaviour noted in previous batch laboratory experiments on other ores can be replicated at scale. In the interests of performing any research and development in a more timely and concise fashion it is also beneficial to have a good idea of the value proposition for the material of interest prior to experimental testing, particularly if throughput is limited by the mills or mining rate.

In addition, it has also been demonstrated that microwave treatment energy doses less than 0.7kWh/t may provide metallurgical benefits for some ores. A lower dose not only reduces the operating cost on an energy consumption basis, but also determines the amount of installed power required and subsequently the maximum throughput for a single treatment module. Such considerations are important for capital expenditure and overall plant complexity. The dose-benefit relationship and apparent rate of diminishing returns for both comminution and separation processes is therefore very important for any economic analysis and project valuation. Hence, it is recommended that ultra-low energy doses (<0.7kWh/t) be considered in future testing campaigns.

Acknowledgements

The authors greatly acknowledge Rio Tinto Technology and Innovation along with their research and industry partners for engagement and collaboration throughout the MicroHammer™ project.

http://dx.doi.org/10.1016/j.mineng.2017.05.003

References

Ali, A.Y., Bradshaw, S.M., 2009. Quantifying damage around grain boundaries in microwave treated ores. Chemical Engineering and Processing: Process Intensification 48, 1566-1573.

Ali, A.Y., Bradshaw, S.M., 2010. Bonded-particle modelling of microwave-induced damage in ore particles. Minerals Engineering 23, 780-790.

Ali, A.Y., Bradshaw, S.M., 2011. Confined particle bed breakage of microwave treated and untreated ores. Minerals Engineering 24, 1625-1630.

Amankwah, R., Khan, A., Pickles, C., Yen, W., 2005. Improved grindability and gold liberation by microwave pretreatment of a free-milling gold ore. Mineral Processing and Extractive Metallurgy 114, 30-36.

Amankwah, R.K., Ofori-Sarpong, G., 2011. Microwave heating of gold ores for enhanced grindability and cyanide amenability. Minerals Engineering 24, 541-544.

Andriese, M.D., Hwang, J.Y., Bell, W., Peng, Z., Upadhyaya, A., Borkar, S.A., 2011. Microwave Assisted Breakage of Metallic Sulfide Bearing Ore, 2nd International Symposium on High-Temperature Metallurgical Processing. Wiley Online Library, pp. 379-386.

Andriese, M.D., Hwang, J.Y., Peng, Z., 2012. Liberation of metallic ‐ bearing minerals from host rock using microwave energy, 3rd International Symposium on High-Temperature Metallurgical Processing. Wiley Online Library, pp. 383-390.

Bailey, C., Lane, G., Morrell, S., Staples, P., 2009. What can go wrong in comminution circuit design?, 10th Mill Operators Conference, Adelaide, Australia, pp. 143-149.

Batchelor, A.R., Jones, D.A., Plint, S., Kingman, S.W., 2015. Deriving the ideal ore texture for microwave treatment of metalliferous ores. Minerals Engineering 84, 116-129.

Batchelor, A.R., Jones, D.A., Plint, S., Kingman, S.W., 2016. Increasing the grind size for effective liberation and flotation of a porphyry copper ore by microwave treatment. Minerals Engineering 94, 61-75.

Bond, F.C., 1961. Crushing and grinding calculations. British Chemical Engineering 6, 378-385.

Bradshaw, S., Louw, W., Van der Merwe, C., Reader, H., Kingman, S., Celuch, M., Kijewska, W., 2007. Techno-economic considerations in the commercial microwave processing of mineral ores. Journal of Microwave Power and Electromagnetic Energy 40, 228-240.

Buttress, A.J., Katrib, J., Jones, D.A., Batchelor, A.R., Craig, D.A., Royal, T.A., Dodds, C., Kingman, S.W., 2017. Towards large scale microwave treatment of ores: Part 1 - Basis of design, construction and commissioning. Minerals Engineering 109, 169-183.

Daniel, M., Lewis-Gray, E., 2011. Comminution efficiency attracts attention. The AusIMM Bulletin 5, 18-28.

Djordjevic, N., 2014. Recovery of copper sulphides mineral grains at coarse rock fragments size. Minerals Engineering 64, 131-138.

Drinkwater, D., Napier-Munn, T.J., Ballantyne, G., 2012. Energy reduction through eco-efficient comminution strategies, 26th International Mineral Processing Congress, IMPC 2012: Innovative Processing for Sustainable Growth-Conference Proceedings. Technowrites, pp. 1223-1229.

FEI, 2016a. Mineral Liberation Analyser (MLA), http://www.fei.com/products/sem/mla/.

FEI, 2016b. QEMScan, https://www.fei.com/products/sem/qemscan/.

Henda, R., Hermas, A., Gedye, R., Islam, M., 2005. Microwave enhanced recovery of nickel-copper ore: communition and floatability aspects. Journal of Microwave Power and Electromagnetic Energy 40, 7-16.

Jones, D.A., Kingman, S.W., Whittles, D.N., Lowndes, I.S., 2005. Understanding microwave assisted breakage. Minerals Engineering 18, 659-669.

Jones, D.A., Kingman, S.W., Whittles, D.N., Lowndes, I.S., 2007. The influence of microwave energy delivery method on strength reduction in ore samples. Chemical Engineering and Processing: Process Intensification 46, 291-299.

Kingman, S., Corfield, G., Rowson, N., 1999. Effects of microwave radiation upon the mineralogy and magnetic processing of a massive Norwegian ilmenite ore. Physical Separation in Science and Engineering 9, 131-148.

Kingman, S.W., Jackson, K., Bradshaw, S.M., Rowson, N.A., Greenwood, R., 2004a. An investigation into the influence of microwave treatment on mineral ore comminution. Powder Technology 146, 176-184.

Kingman, S.W., Jackson, K., Cumbane, A., Bradshaw, S.M., Rowson, N.A., Greenwood, R., 2004b. Recent developments in microwave-assisted comminution. International Journal of Mineral Processing 74, 71-83.

Kingman, S.W., Vorster, W., Rowson, N.A., 2000a. The effect of microwave radiation on the processing of Palabora copper ore. Journal of the South African Institute of Mining and Metallurgy 100, 197-204.

Kingman, S.W., Vorster, W., Rowson, N.A., 2000b. The influence of mineralogy on microwave assisted grinding. Minerals Engineering 13, 313-327.

Kojovic, T., Michaux, S., Walters, S., 2010. Development of new comminution testing methodologies for geometallurgical mapping of ore hardness and throughput, Proceedings 25th IMPC, Brisbane, Australia, pp. 891-899.

Kumar, A., Ramaro, V., Kamath, B.P., Ray, K., Km, K., 2006. Energy reduction in ore comminution through microwave, Sohn International Symposium; Advanced Processing of Metals and Materials Volume 4: New, Improved and Existing Technologies: Non-Ferrous Materials Extraction and Processing, pp. 481-489.

Kumar, P., Sahoo, B.K., De, S., Kar, D.D., Chakraborty, S., Meikap, B.C., 2010. Iron ore grindability improvement by microwave pre-treatment. Journal of Industrial and Engineering Chemistry 16, 805-812.

Like, Q., Jun, D., 2016. Analysis on the growth of different shapes of mineral microcracks in microwave field. Frattura ed Integritá Strutturale, 342-351.

Marion, C., Jordens, A., Maloney, C., Langlois, R., Waters, K.E., 2016. Effect of microwave radiation on the processing of a Cu ‐ Ni sulphide ore. The Canadian Journal of Chemical Engineering 94, 117-127.

Omran, M., Fabritius, T., Mattila, R., 2015. Thermally assisted liberation of high phosphorus oolitic iron ore: A comparison between microwave and conventional furnaces. Powder Technology 269, 7-14.

Orumwense, A., Negeri, T., 2004. Impact of microwave irradiation on the processing of a sulfide ore. Minerals and Metallurgical Processing 21, 44-51.

Pokrajcic, Z., Morrison, R., Johnson, B., 2009. Designing for a reduced carbon footprint at Greenfield and operating comminution plants, Recent Advances in Mineral Processing Plant Design. Society for Mining, Metallurgy, and Exploration, pp. 560-570.

Powell, M., Bye, A., 2009. Beyond mine-to-mill: Circuit design for energy efficient resource utilisation, Tenth Mill Operators Conference 2009, Proceedings. AusIMM, pp. 357-364.

Rizmanoski, V., 2011. The effect of microwave pretreatment on impact breakage of copper ore. Minerals Engineering 24, 1609-1618.

Sahyoun, C., Rowson, N., Kingman, S., Groves, L., Bradshaw, S., 2005. The influence of microwave pre-treatment on copper

http://dx.doi.org/10.1016/j.mineng.2017.05.003

flotation. Journal of the South African Institute of Mining and Metallurgy 105, 7-14.

Salsman, J.B., Williamson, R.L., Tolley, W.K., Rice, D.A., 1996. Short-pulse microwave treatment of disseminated sulfide ores. Minerals Engineering 9, 43-54.

Scott, G., Bradshaw, S.M., Eksteen, J.J., 2008. The effect of microwave pretreatment on the liberation of a copper carbonatite ore after milling. International Journal of Mineral Processing 85, 121-128.

Vorster, W., Rowson, N.A., Kingman, S.W., 2001. The effect of microwave radiation upon the processing of Neves Corvo copper ore. International Journal of Mineral Processing 63, 29-44.

Walkiewicz, J., Lindroth, D., Clark, A., 1993. Grindability of taconite rod mill feed enhanced by microwave-induced cracking. PREPRINTS-SOCIETY OF MINING ENGINEERS OF AIME.

Walkiewicz, J.W., Clark, A.E., McGill, S.L., 1991. Microwave-assisted grinding. IEEE Transactions on industry applications 27, 239-243.

Wang, G., Radziszewski, P., Ouellet, J., 2008. Particle modeling simulation of thermal effects on ore breakage. Computational Materials Science 43, 892-901.

Wang, Y., Djordjevic, N., 2014. Thermal stress FEM analysis of rock with microwave energy. International Journal of Mineral Processing 130, 74-81.

Wang, Y., Forssberg, E., 2005. Dry comminution and liberation with microwave assistance. Scandinavian Journal of Metallurgy 34, 57-63.

Whittles, D.N., Kingman, S.W., Reddish, D.J., 2003. Application of numerical modelling for prediction of the influence of power density on microwave-assisted breakage. International Journal of Mineral Processing 68, 71-91.

http://dx.doi.org/10.1016/j.mineng.2017.05.003

Supplementary Data

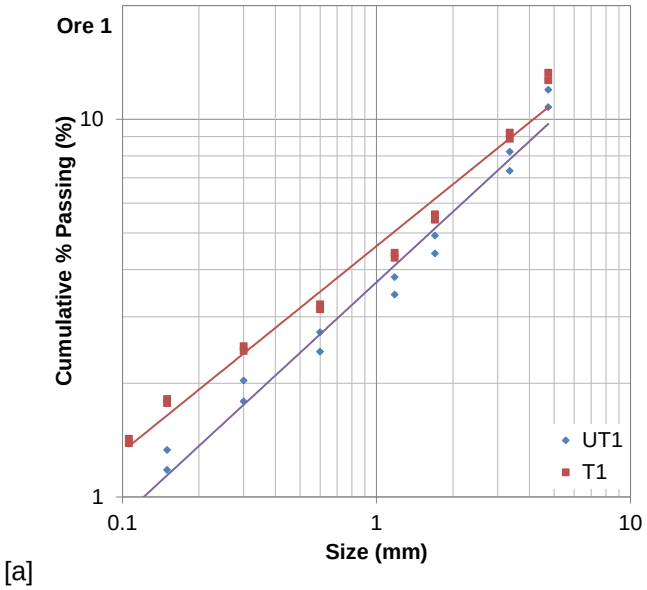

[a]

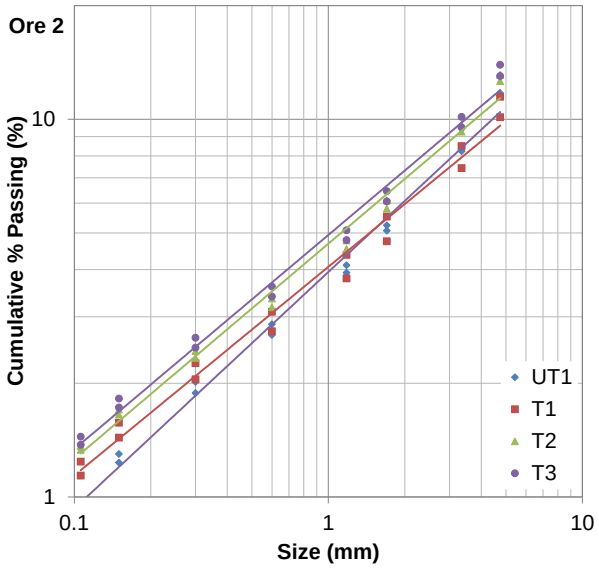

[b]

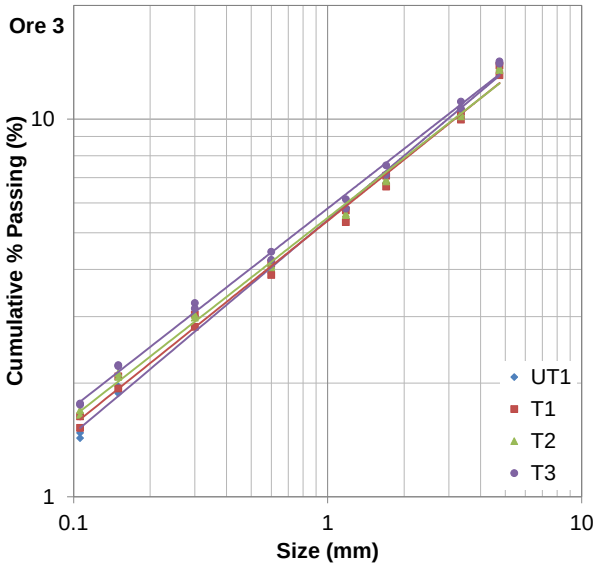

[c]

Figure S.1: Phase I JKGeM Ci test sizings for [a] Ore 1, [b] Ore 2 and [c] Ore 3

http://dx.doi.org/10.1016/j.mineng.2017.05.003

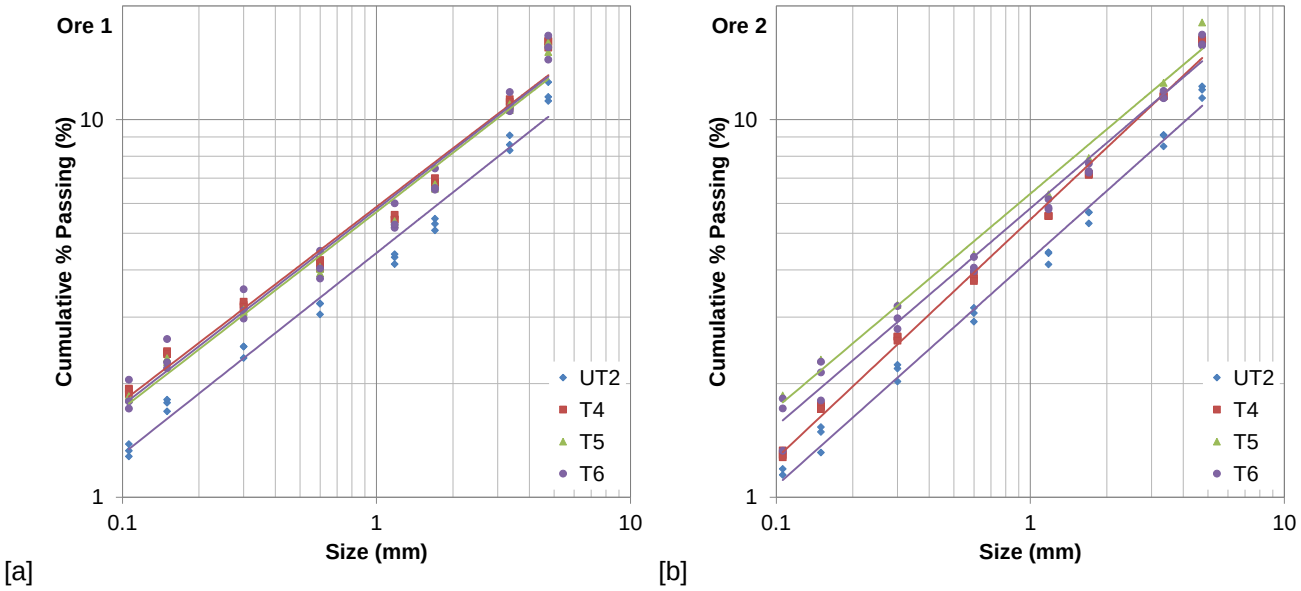

Figure S.2: Phase II JKGeM Ci test sizings for [a] Ore 1 and [b] Ore 2

http://dx.doi.org/10.1016/j.mineng.2017.05.003

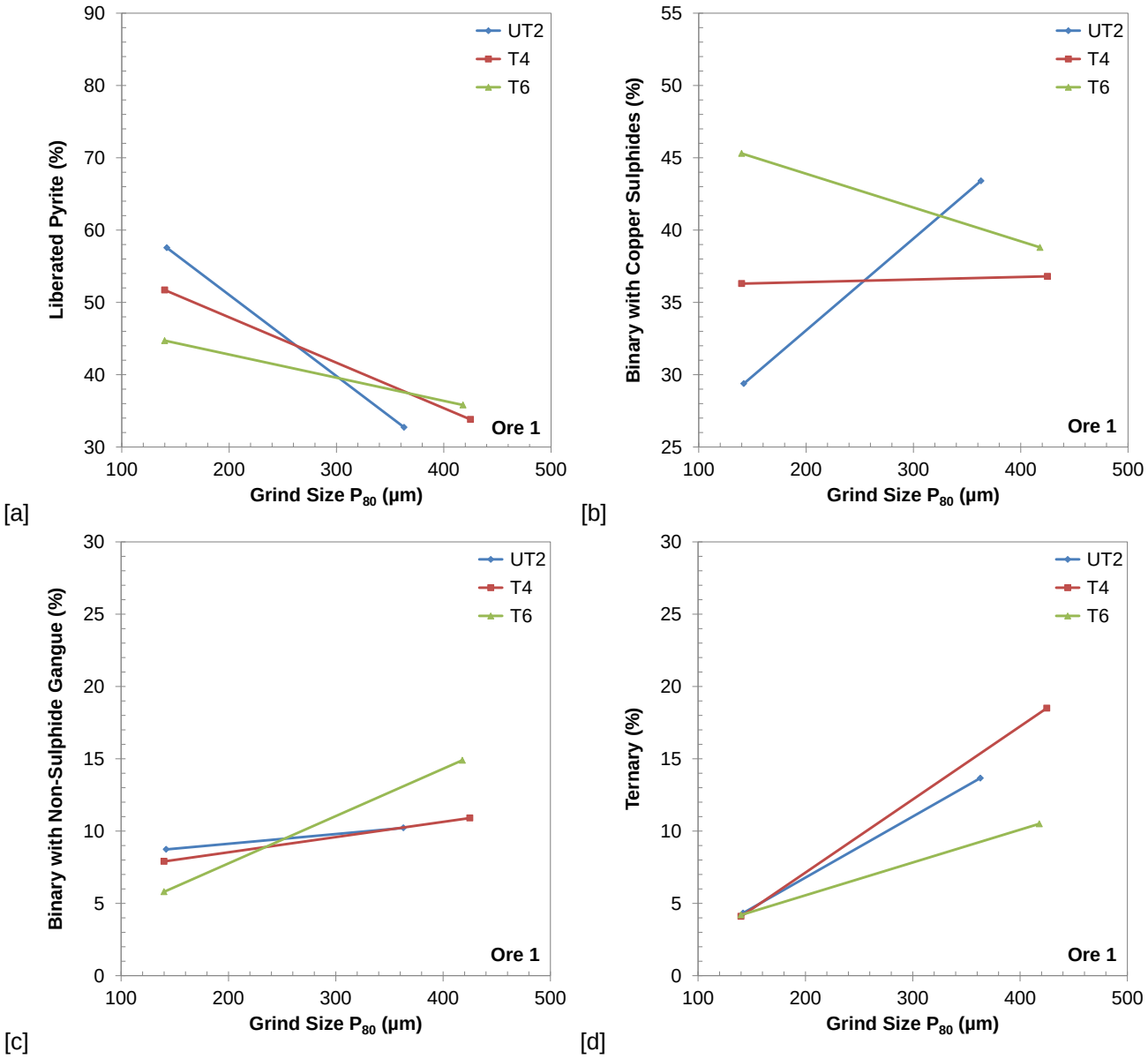

Figure S.3: Phase II Ore 1 pyrite locking data (5% tolerance) [a] liberated, [b] binary with copper sulphide, [c] binary with non-sulphide gangue, and [d] ternary

http://dx.doi.org/10.1016/j.mineng.2017.05.003

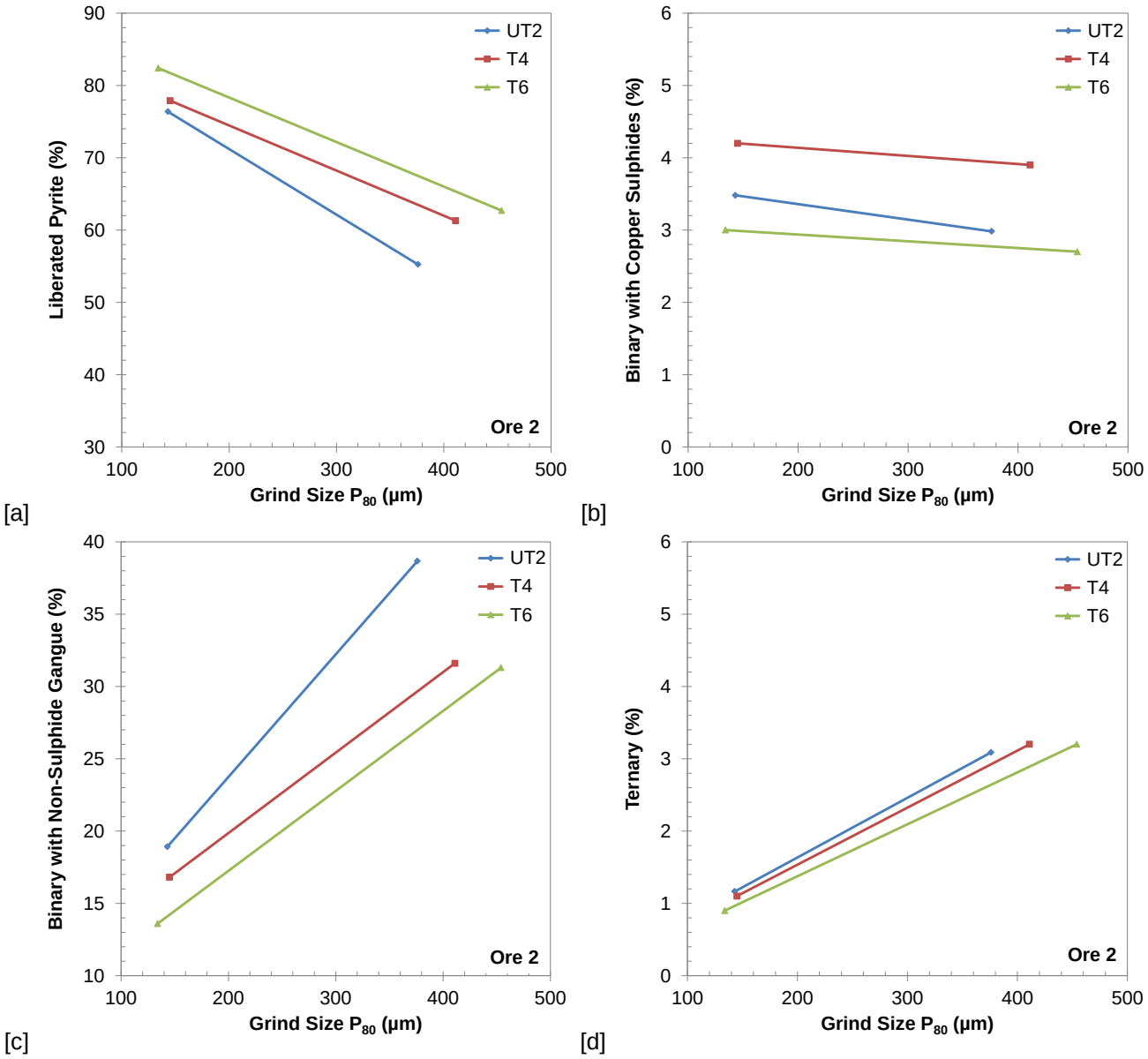

Figure S.4: Phase II Ore 2 pyrite locking data (5% tolerance) [a] liberated, [b] binary with copper sulphide, [c] binary with non-sulphide gangue, and [d] ternary

http://dx.doi.org/10.1016/j.mineng.2017.05.003